The University of Manitoba

THE HIGH RESOLUTION PROTON MAGNETIC RESONANCE STUDY OF TRIPTYCENE

presented by

Kevin Glen Kidd

A Thesis
Submitted to
the Faculty of Graduate Studies and Research
University of Manitoba
In partial Fulfillment
of the Requirements for the Degree
MASTER OF SCIENCE

Winnipeg, Manitoba
September, 1966

ACKNOWLEDGEMENTS

The research work constituting this thesis has been carried out at the suggestion of Dr. T. Schaefer and under his guidance. I would like to thank him for his help and for his patience.

The progress of my research was made considerably easier by the generous advice of George Kotowycz and Drs. H. Hutton and F. Hruska. For this I am grateful, and also for many stimulating discussions.

In addition I wish to express my gratitude to the National Research Council for the provision of financial support.

ABSTRACT

The triptycene AA'BB' nuclear magnetic resonance spectrum is analyzed. The proton shifts relative to internal tetramethyl silane are determined to be 2.80 p.p.m. (on the τ scale) for one class of ring protons and 3.14 p.p.m. for the other. The coupling constants for the system are determined: 7.58 and 7.21 cycles/sec. for ortho couplings between equivalent and nonequivalent protons, respectively, 1.22 cycles/sec. for meta coupling and 0.57 cycles/sec. for para coupling.

The best predicted values for the chemical shifts of ring protons 2.83 p.p.m. and 3.08 p.p.m. are obtained on the basis of ring current tables and approximate substituent effects.

The proton shift relative to internal tetramethyl silane for the bridgehead hydrogens is 4.79 p.p.m. on the τ scale. A value for the C^{13}-H coupling constant of the bridgehead hydrogen is predicted to fall near the range 146 - 150 cycles/sec.

TABLE OF CONTENTS

Chapter		Page
I	INTRODUCTION	1
	A - The Nuclear Magnetic Resonance Theory. .	1
	B - The Nuclear Magnetic Resonance Method. .	9
II	THE CHEMICAL SHIFT	15
	A - The Theory of the Shielding Constant . .	15
	B - The Effect of Anisotropy on the Shielding Constant	22
	C - Interatomic Currents	28
	1. Development of the Ring Current Theory.	28
	2. Application of the Ring Current Theory.	34
III	THE COUPLING CONSTANT	38
	A - The Theory of the Coupling Constant. . .	38
	B - Coupling Constant in the Aromatic Ring. .	41
IV	ANALYSIS OF THE AA'BB' SPECTRUM	43
V	ANISOTROPY AND C^{13}-H COUPLING CONSTANTS. . .	54
VI	THE NATURE OF THE PROBLEM.	58
VII	EXPERIMENTAL METHODS	60
VIII	EXPERIMENTAL RESULTS	61
	A - Triptycene Ring Proton	72

Chapter Page

B - Bridgehead Protons 78

C - Benzene 78

IX DISCUSSION OF RESULTS 79

A - Introduction 84

B - The Chemical Shift of the Ring Protons . 85

C - C^{13}-H Coupling Constant of the Bridge-head Group 91

X SUMMARY AND CONCLUSIONS 94

APPENDIX A 96

APPENDIX B 103

BIBLIOGRAPHY 105

LIST OF TABLES

Table		Page
I	Summary of transitions and intensities . . .	47
II	Intensities and energies relative to the center of the band AA'BB' portion of the triptycene spectrum	66
III	Comparison of parameters evaluated by different combinations of line energies (an internal check).	67
IV	Evaluation of C, D, F, G and $\nu_o \delta$	68
V	Evaluation of N, K, L and M	68
VI	Summary of the chemical shift and coupling constants	69
VII	Comparison of theoretical and observed intensities	70
VIII	Partial AA'BB' spectrum, calculated and experimental	71
IX	Comparison of the analysis obtained in this work with the results of Smith and Shoulders (55)	81
X	Electron densities of the π electron system of triptycene (from Appendix A)	82
XI	Prediction of the chemical shift of the ring protons of triptycene	83
XII	p-π symmetry orbitals	100
XIII	Electron densities in the carbon p-π orbitals	101

Table Page

XIV Coordinate positions for all classes of triptycene hydrogen relative to an origin on one of the rings 103

XV Shielding at the different classes of protons in triptycene 104

LIST OF FIGURES

Figure		Page
1.	Nuclear spin model	1
2.	Nuclear spin model	3
3.	The nucleus in a magnetic field. . . .	4
4.	Energy levels for I = 1/2	5
5.	Precession of the nuclear magnetic moment	6
6.	A comparison of the chemical shifts on the δ and τ scales	14
7.	Protons with sp^2 hybridization	20
8.	Effect of the field due to a neighbouring point dipole	25
9.	Magnetic field produced by ring current	30
10.	Comparison of calculated ring current shifts with experimental values. . . .	35
11.	Coupling in a crystalline lattice. . .	39
12.	Coupling in a liquid or gaseous phase	40
13.	Coupling for an AA'BB' system.	48
14.	The triptycene molecule.	59
15a.	Simple spectrum of triptycene.	61
15b.	Decoupled spectrum of triptycene . . .	61
16.	Possible line assignments for triptycene	62
17.	Line assignment of triptycene spectrum	63
18.	Chemical shifts of the A and B portion of the triptycene spectrum	64

Figure		Page
19.	Calculated and experimental triptycene spectra	65
20b.	Triptycene: definition of terms	69
20.	Assignment of triptycene ring protons .	75
21.	Experimental and predicted values for the chemical shifts of the ring proton	79
22.	Steric hindrance of ring protons . . .	79a
23.	The proton chemical shift plotted as a function of C^{13}-H coupling to the proton	80
24.	Numbering system of carbon atomic orbitals	97
25.	Inter-ring overlap of Class I p orbitals	101
26.	Energy level diagram of the p-π electron system of triptycene	102

Chapter I

INTRODUCTION

A - THE NUCLEAR MAGNETIC RESONANCE THEORY

The nuclear magnetic resonance method is described in a number of reference works (1, 2, 3). As in the quantum theory of electronic energy levels in which the electron is assigned a spin, certain nuclei are assigned an intrinsic spin angular momentum. In classical terms this implies a circulation of mass about an axis and is depicted as a vector quantity $\underline{a}$ (Figure 1).

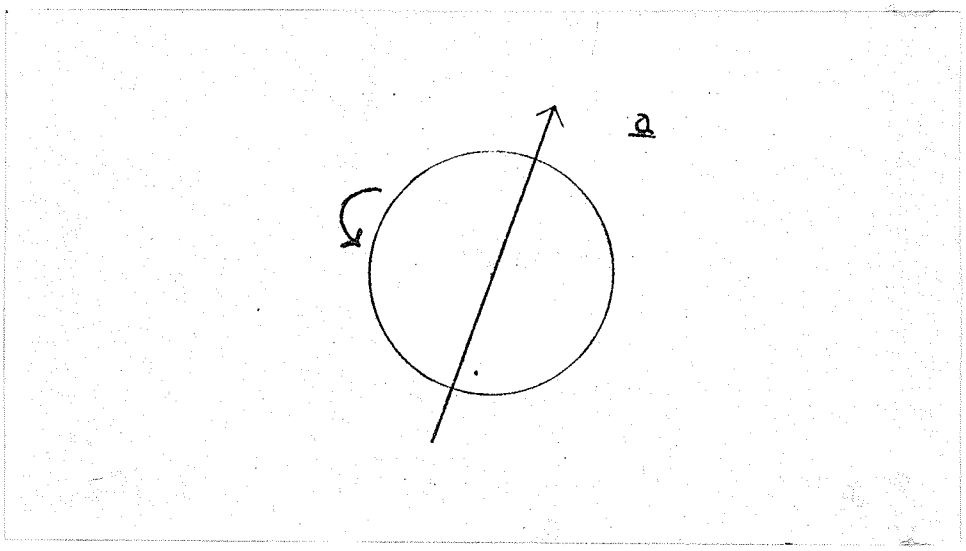

Figure 1: Nuclear spin model

The quantum theory of matter requires that there be a limited number of angular momentum states in which the system can exist. It is not possible to describe a "state" by giving the direction of its angular momentum, but only by giving the component of the angular momentum

along some arbitrary direction commonly taken as the z axis. Quantum mechanically, the angular momentum is quantized according to the equation

$$(1) \qquad a_z = m\hbar$$

where $m = I, (I - 1), \ldots 0, \ldots -(I - 1), -I$

$\hbar = \frac{h}{2\pi}$ and h is Planck's constant

a_z is the z component of the angular momentum and

I is integral or half integral.

In the classical model the angular momentum is represented by the vector $\underline{a}$ of magnitude

$$(2) \qquad |\underline{a}| = \sqrt{I(I + 1)}\ \hbar$$

and can assume only the orientations which give the above z components.

The classical model treats the nucleus as a charged particle. If the nucleus possesses a spin, there is also a circulation of charge which generates a magnetic moment. This magnetic moment is represented by a vector $\underline{\mu}$ which lies along $\underline{a}$ (Figure 2). Classical calculations on atomic hydrogen yield

$$(3) \qquad \underline{\mu} = \left(\frac{q_p}{2m_p c}\right) \underline{a}$$

where q_p is the charge of the proton

m_p is the mass of the proton

c is the velocity of light

The correct relation, however, is found to be

$$(4) \qquad \underline{\mu} = g \left(\frac{q_p}{2m_p c}\right) \underline{a}$$

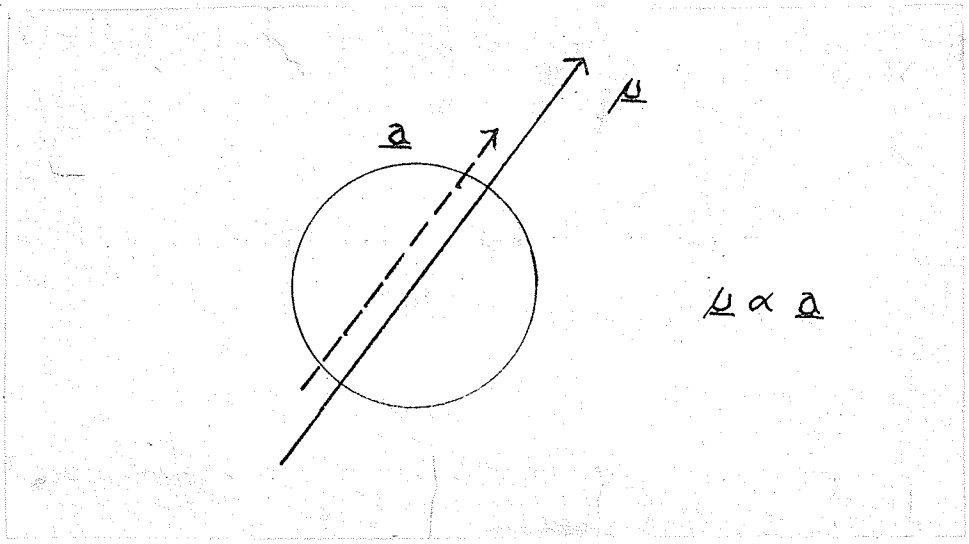

Figure 2: Nuclear spin model

where g is the nuclear g factor corresponding to the Landé factor. An alternative expression is

$$(5) \qquad \underline{\mu} = \gamma \underline{a}$$

where $\gamma = g\left(\frac{q_p}{2m_p c}\right)$ is the magnetogyric ratio. It follows, then, that

$$(6a) \qquad |\underline{\mu}| = g\left(\frac{q_p}{2m_p c}\right)\sqrt{I(I+1)}\ \hbar$$

$$(6b) \qquad |\underline{\mu}| = g\mu_o\sqrt{I(I+1)}$$

where μ_o is the Bohr magneton $\frac{q_p \hbar}{2m_p c}$.

In the absence of a magnetic field, the orientation of the vector $\underline{\mu}$ will not have any effect on the energy of

the nucleus. The angular momentum states are degenerate and equally populated. In the presence of an applied magnetic field $\underline{H}^{o}$, however, there is an energy of interaction between the magnetic moment of the nucleus and the field (Figure 3).

(7) $$E = -\underline{\mu} \cdot \underline{H}^{o} = -\mu H^{o} \cos\theta = -\mu_{z} H^{o}$$

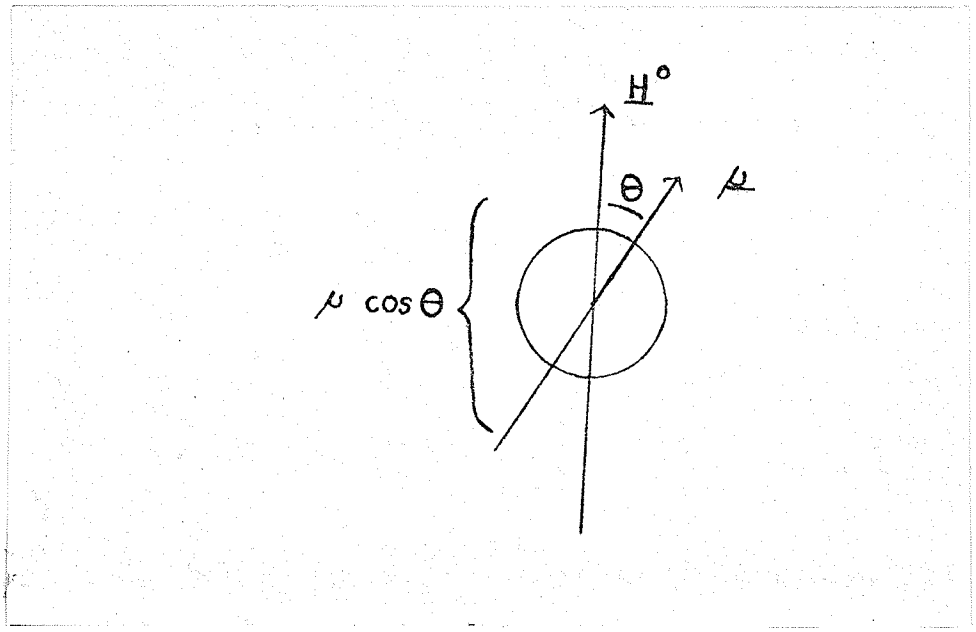

Figure 3: The nucleus in a magnetic field

The nuclear magnetic moment is quantized corresponding to the angular momentum. Thus the z component of the magnetic moment vector can take on only certain values (equation 1).

(1) $$a_{z} = m\hbar$$

where $m = I, (I - 1), \ldots -(I - 1), -I$

and (8) $$\mu_{z} = mg\mu_{o}.$$

It is apparent that the energy of interaction is quantized. In the case ofthe hydrogen nucleus the nuclear spin or angular momentum is 1/2. Then

(9) $I = 1/2$

(10) $m = \pm 1/2$

(11) $E_{+\frac{1}{2}} = -1/2\ g\mu_0 H^0$

(12) $E_{-\frac{1}{2}} = +1/2\ g\mu_0 H^0$.

The two proton spin states are rendered non-degenerate by the application of a magnetic field and are separated by the energy difference $g\mu_0 H$. In the classical model these two states are depicted as two orientations of the spin vector (Figure 4).

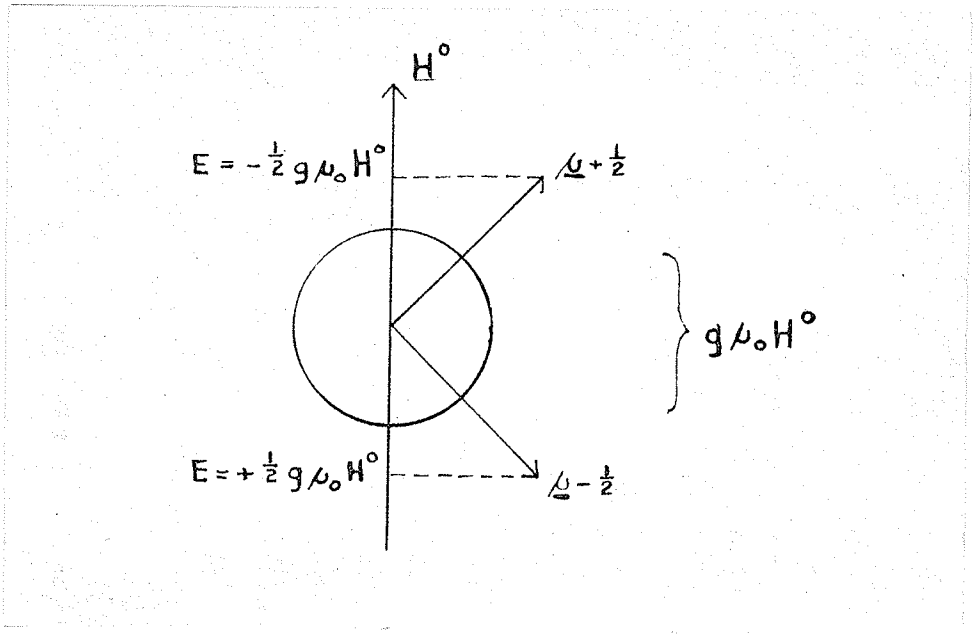

Figure 4: Energy levels for I = 1/2

A temperature dependent equilibrium exists between the spin states as determined bythe Boltzmann

factor. Transitions, however, may be induced between the energy levels by the application of a magnetic field oscillating in the radiofrequency region. Application of the relation

$$\Delta E = h\nu \tag{13}$$

to this case gives

$$h\nu = g\mu_o H^o \tag{14a}$$

$$= \frac{g\mu_o H^o}{h} \tag{14b}$$

where ν is the frequency associated with the energy transfer and hence the resonance frequency. Application of a source of energy of the same frequency as the resonance frequency is accompanied by an exchange of energy and gives the resonance peak observed in the nuclear magnetic resonance method.

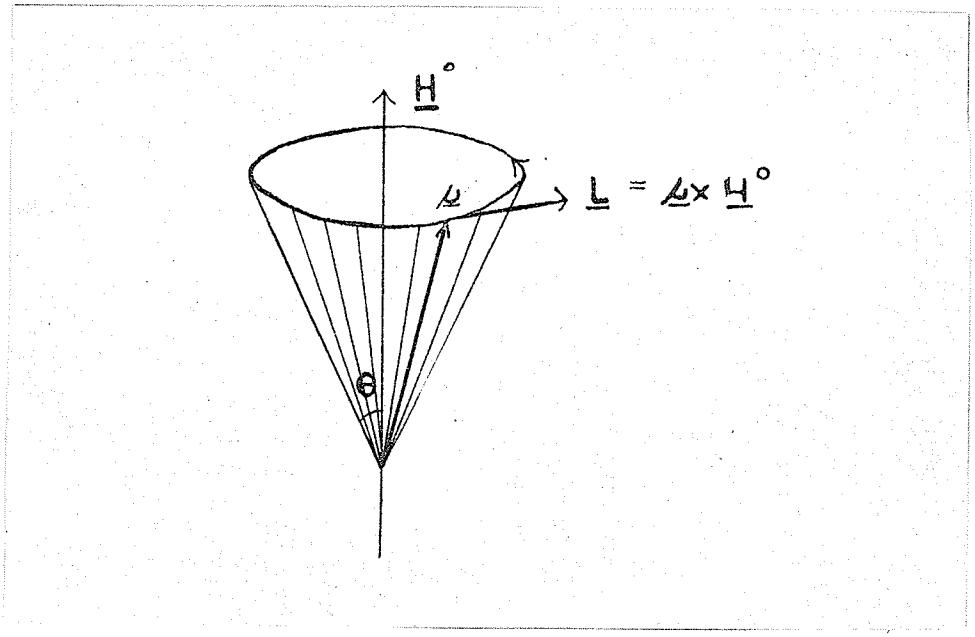

Figure 5: Precession of the nuclear magnetic moment

The resonance condition may also be explained in terms of the classical model. There is a permanent torque $\underline{L}$ acting on the nucleus.

$$(15) \qquad \underline{L} = \underline{\mu} \times \underline{H}^{o}$$

Since the magnetic moment vector $\underline{\mu}$ lies along the spin vector $\underline{a}$, the torque produces a precession of the vector $\underline{\mu}$ about the z axis (Figure 5). The rate of precession of the magnetic moment is related to the torque by the relation

$$(16) \qquad \frac{d\underline{a}}{dt} = \underline{L} = \underline{\mu} \times \underline{H}^{o}.$$

With equation (5) this result may be expressed

$$(17) \qquad \frac{d\underline{\mu}}{dt} = \gamma(\underline{\mu} \times \underline{H}^{o}).$$

The angular velocity of the precession is then given by

$$(18) \qquad \omega \text{ (in radians/sec.)} = \frac{2\pi \left| d\underline{\mu}/dt \right|}{2\pi \mu \sin\theta} = \gamma H^{o}.$$

If in addition to the magnetic field $\underline{H}^{o}$, a second, smaller, magnetic field $\underline{H}_{1}$ is applied perpendicular to the principal field $\underline{H}^{o}$ there will be a second torque acting on the magnetic moment $\underline{\mu}$. The effect of this torque is to induce precession about an axis perpendicular to the field $\underline{H}^{o}$. Due to the rapid precession of $\underline{\mu}$ about the field $\underline{H}^{o}$, the incoherent direction of the torque due to $\underline{H}_{1}$ produces only a slight wobble in the precession of $\underline{\mu}$. If the applied field $\underline{H}_{1}$ is an oscillating field of frequency $\omega_{1} = \gamma H^{o}$, then the effect of this field is in

phase with the precession about $\underline{H}^{o}$, and the constantly directed torque can flip the magnetic moment to another of its "states" or orientations. This condition, the resonance condition, is thus marked by a transfer of energy.

B - THE NUCLEAR MAGNETIC RESONANCE METHOD

The experimental nuclear magnetic resonance method consists of a sample placed in a large magnetic field $\underline{H}^o$, the precession of the nuclear magnetic moments $\underline{\mu}_i$ at a rate ω_i determined by the field $\underline{H}^o$, and the application of an oscillating magnetic field perpendicular to $\underline{H}^o$. To observe the resonance condition in a nuclear species i, the frequency of the oscillating field must equal ω_i. The two methods for obtaining the resonance condition are: a) varying the frequency of the applied oscillating field until it is equal ω_i; b) varying the main field $\underline{H}^o$ in magnitude thus altering the precession frequency ω_i to equal the fixed frequency of the oscillating field which is the resonance frequency.

On the basis of this classical model, the frequency of precession ω of a nuclear magnetic moment $\underline{\mu}_i$ is expected to be

$$\omega_i = \gamma_i H^o \qquad (19)$$

where γ_i is dependent on $|\underline{\mu}|$. This however is applicable only to the case of a bare nucleus. In the physical situation encountered in actual measurements, the nuclei under study are surrounded by electrons. The applied field $\underline{H}^o$ creates diamagnetic currents in this electron cloud, and an induced field $\underline{H}'$ is generated which is opposed to the applied field. The induced field is proportional to the applied field

$$(20) \qquad \underline{H}' = -\sigma_i \underline{H}^o$$

where σ_i is the shielding constant and is characteristic of atom i and its nucleus. The nucleus is shielded and the effective field $\underline{H_{eff}}$ at the nucleus is

$$(21a) \qquad (\underline{H_i})_{eff} = \underline{H}^o + \underline{H}_i'$$

$$(21b) \qquad (\underline{H_i})_{eff} = \underline{H}^o (1 - \sigma_i).$$

This shielding constant is, to a large extent, dependent upon the electron density of the electron cloud surrounding the nucleus. The electron density in two identical atoms in different chemical situations - the methyl protons and the alcoholic proton in CH_3OH for example - is obviously different due to the electronegativity of the atom to which each type of nucleus is bound. The shielding coefficient for such nuclei is different. Precession frequencies are no longer given by

$$(19) \qquad \omega_i = \gamma_i H^o$$

but instead by

$$(22) \qquad \omega_i = \gamma_i (H_i)_{eff} = \gamma_i H^o (1 - \sigma_i)$$

with the result that the resonance frequency for nuclei with different σ_i is also different. Whether the spectrum is taken by the field sweep method or by the frequency sweep method, the resonance lines will occur at different positions. Nuclei which are chemically different and distinguishable show up as distinct resonance lines.

The separation between the lines is defined as the chemical shift δ. The field sweep method measures line positions in gauss or milligauss and gives the chemical shift in milligauss. Alternatively the shift could have been obtained by the frequency sweep method, giving a result in cycles/second. Since the value of the field and the frequency at resonance are interconvertible, the result in milligauss may be converted to cycles/second by

$$(23) \qquad \delta\,(\text{cycles/sec.}) = \frac{\gamma}{2\pi}\delta\,(\text{milligauss}) = \frac{\gamma}{2\pi}(H_2 - H_1)$$

The chemical shift in cycles per second is given by

$$(24) \qquad \delta = \frac{\gamma}{2\pi}H^{\circ}(\sigma_2 - \sigma_1)$$

where the shielding constant represents in effect the chemical shift of the particular proton from the resonance position of the bare proton. Since the latter is an impractical reference point, all chemical shifts are listed relative to an arbitrarily chosen standard, the most common standard being the resonance line of tetramethyl silane, $Si(CH_3)_4$. The "standard" chemical shift of nucleus i refers to

$$(25) \qquad \delta_i = \frac{\gamma}{2\pi}H^{\circ}(\sigma_r - \sigma_i)$$

where σ_r is the shielding constant of the reference proton.

Thus there exist the two systems of units in which the shift δ_i may be measured:

(26a) δ_i (in milligauss) $= H_i - H_r = H^o(\sigma_r - \sigma_i)$

(26b) δ_i (in cycles/sec) $= \nu_r - \nu_i = \frac{\gamma}{2\pi} H^o(\sigma_r - \sigma_i)$

$= \nu^o(\sigma_r - \sigma_i)$

Both of the equations exhibit the principle difficulty inherent in these systems. The chemical shift is directly proportional to: a) the applied field or b) the applied frequency. A simplification occurs ifthe first equation is divided by H^o(which is the field at which a bare nucleus, $\sigma = 0$, resonates). The corresponding operation on equation (26b) is to divide by $\frac{\gamma}{2\pi} H^o$ (which is the frequency at which a bare nucleus resonates). In the first case the result is expressed as the ratio of the shift in milligauss to the applied field (which is normally of the order of 10,000 gauss), giving the chemical shift in parts per million (p.p.m.) of the applied field. In the second case the result is expressed as the ratio of the shift in cycles per second to the operating frequency. Again the chemical shift is in parts per million. The numerical result obtained by either procedure is identical, as is readily verified from (26a) and (26b).

(27) δ_i (p.p.m.) $= \sigma_r - \sigma_i$

A modification is made in actual calculations. δ in parts per million is given by

$$(28) \qquad \delta = \frac{H^{o}(\sigma_r - \sigma_i)}{H^{o}} = \frac{H_r - H_i}{H^{o}} .$$

H^{o} is not an easily obtainable experimental value and H_r is substituted for H^{o} since in absolute magnitude the two quantities are very close. The chemical shift is calculated from

$$(29) \qquad \delta_i = \frac{H_r - H_i}{H_r} .$$

The term $\frac{\gamma}{2\pi} H^{o}$ or ν^{o} is more easily determined and the alternative calculation for δ is

$$(30) \qquad \delta_i = \frac{\nu_r - \nu_i}{\nu^{o}} .$$

In the system for calculating chemical shifts outlined above tetramethyl silane has a shift of zero by definition, and classes of protons resonating to low field have positive (or greater) values for the chemical shift. This results in a seeming contradiction in terms, and another system, the τ system, is frequently employed. On the τ scale the chemical shift of tetramethyl silane is defined equal to 10 with other resonances listed in decreasing values in p.p.m. on the τ scale according to

$$(31) \qquad \tau = 10 - \delta .$$

A comparison of the two systems is given in Figure 6.

Chapter II

THE CHEMICAL SHIFT

A - THE THEORY OF THE SHIELDING CONSTANT

In the classical formulation of the nuclear magnetic resonance method, the nucleus is considered to possess a magnetic moment. In this model the motion of the magnetic moment is determined by the magnitude of the external magnetic field at the nucleus. For the unshielded nucleus this is simply the magnitude of the external field less the diamagnetic or paramagnetic effect of any intervening medium. In the case of the nuclei surrounded by a normal electron configuration there is an additional net diamagnetic shielding due to electronic motion.

Of obvious interest to the nuclear magnetic resonance method is the ability to formulate theoretically this electronic shielding. Mathematical calculations were carried out for an atom in the ^1S state by Lamb (4). His results showed that the diamagnetic effect on an atom in the ^1S state could be represented by a magnetic field $\underline{H}'$ opposed to the applied field $\underline{H}^o$. The vector potential $\underline{A}$ of an electron may be expressed by

$$(32) \qquad \underline{A} = 1/2 \left[\underline{H}^o \times \underline{r}\right]$$

where $\underline{H}^o$ = applied field and $\underline{r}$ = position of the electron. This gives rise to a diamagnetic current and induced field given by

$$(33a) \qquad \underline{H}' = -\frac{e^2\underline{H}^o}{3mc^2}\int\frac{\rho(r)}{r}\,d\tau$$

$$(33b) \qquad \underline{H}' = -\frac{4\pi e^2\underline{H}^o}{3mc^2}\int r\rho(r)\,dr$$

where $\rho(r)$ = electron density at radius r from the nucleus

$d\tau$ = differential volume element

dr = differential radius element

This method requires only an evaluation of the integral $\int r\rho(r)\,dr$, that is, a knowledge of the electron wave function.

In the equivalent notation of Lamb's theory involving the shielding constant

$$(21b) \qquad \underline{H} \equiv \underline{H}^o(1-\sigma)$$

where $\underline{H}$ = resultant field at the nucleus and σ = the shielding constant. A comparison indicates that

$$(20) \qquad \underline{H}' = -\sigma\underline{H}^o$$

and

$$(34) \qquad \sigma = \frac{4\pi e^2}{3mc^2}\int_o^\infty r\rho(r)\,dr.$$

The ^1S state is characterized by spherical symmetry. Lamb's theory therefore is applicable only to free atoms since it depends on the spherical symmetry of the electric field of the nuclear electrical potential. It is evident that another treatment is necessary to handle the case of a nucleus in a polyatomic molecule. The corresponding calculations for the molecular case are more complex. A second order calculation of the shielding

constant for a nucleus in a polyatomic molecule was given by Ramsey (5, 6).

As was shown above the magnetic field under conditions of spherical symmetry is relatedto the applied field by a simple proportionality. In the absence of spherical symmetry, this relation does not necessarily hold. Both the applied and induced fields are vector magnitudes, and the induced field $\underline{H}'$ need not lie parallel to the applied field $\underline{H}^o$. In such a case, the expression for the induced field is

$$(20) \qquad \underline{H}' = -\underline{\sigma}\,\underline{H}^o$$

and the screening coefficient, $\underline{\sigma}$, is not a constant, but a second rank tensor.

Ramsay in his treatment takes as the vector potential $\underline{A}_{k\lambda}$.

$$(35) \qquad \underline{A}_{k\lambda} = 1/2\ \underline{H}^o \times \underline{r}_k + \underline{\mu} \times \underline{r}_k/r_k^3 - 1/2\ \underline{H}^o \times \underline{R}_{k\lambda}$$

where k refers to the k th electron

λ refers to the molecular orientation

$\underline{r}_k$ is the position of the k th electron

$\underline{R}_{k\lambda}$ is a constant arising from the arbitrariness of the gauge of the vector potential

$\underline{\mu}$ is the magnetic moment of the nucleus under consideration.

The general form of the shielding tensor obtained by perturbation theory is composed of two terms which may

be identified as a diamagnetic term and a paramagnetic term. The diamagnetic term, similar to the Lamb equation, represents the effect of an hypothetical spherically symmetrical distribution of the electrons of the molecule about the nucleus in question, while the paramagnetic term takes account of the lack of spherical symmetry. A calculation of the shielding constant (after averaging over all orientations of the molecule) from this general expression for $\underline{\sigma}$ is not practical, however, since it would require a knowledge of the excited state wave functions and in general these are not known. The Ramsey formula may be simplified to an approximate form after the manner used by Van Vleck and Frank (7) in a similar calculation on the diamagnetic susceptibility of molecular hydrogen. The simpler form contains only ground state wave functions, however, it involves the second derivatives and is very sensitive to any errors in the wave functions chosen.

The discussion of the Ramsey method indicates that for anything more complicated than the simplest

molecules, a calculation of the chemical shifts of substituent nuclei from basic principles is at present not possible. Attempts have been made, therefore, to divide the shielding constant into contributions from electrons localized on atoms and in chemical bonds (7, 8). The shielding constant σ_A for nucleus A in a molecule is written as

$$(36) \qquad \sigma_A = \sigma_{AA}^{dia} + \sigma_{AA}^{para} + \sum_{B \neq A} \sigma_{AB} + \sigma_A^{deloc}$$

where σ_{AA}^{dia} is due to induced diamagnetic currents on atom A

σ_{AA}^{para} is due to induced paramagnetic currents on atom A

σ_{AB} is due to local induced currents on the atoms other than A

σ_A^{deloc} is due to interatomic circulations of electrons

The value of the above equation is evident in comparing the chemical shifts of nuclei in different compounds. If two nuclei are characterized by identical or equivalent electron shells, the first two terms σ_{AA}^{dia} and σ_{AA}^{para} would be the same for both nuclei. Consider, for example, the proton resonance spectrum of benzene and ethylene (Figure 7). The carbon atom involved in the C-H bond has sp^2 hybridization in both cases and the localized electron shell of the hydrogen atom is the same. Any difference observed in the

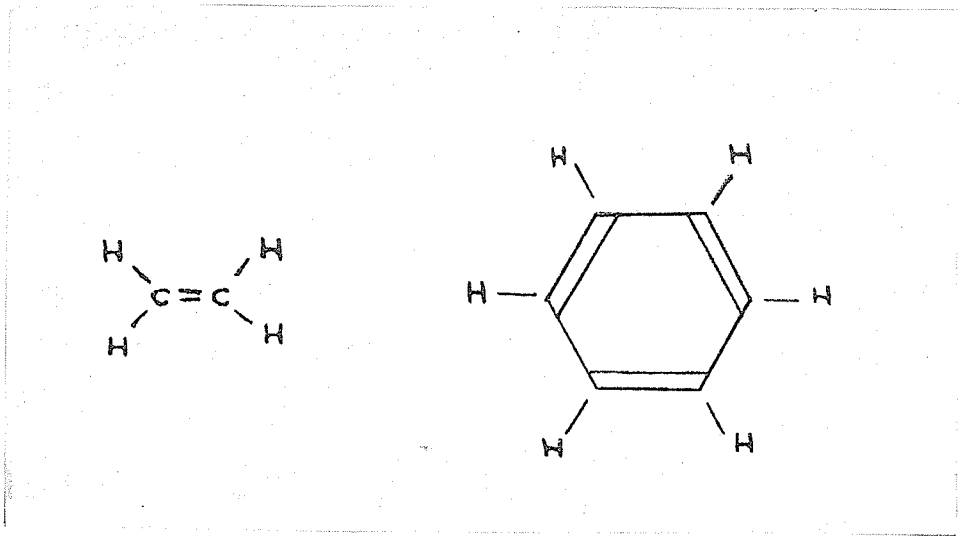

Figure 7: Protons with sp^2 hybridization

chemical shift of the two associated nuclei is attributed to the last terms of the equation, $\sum_{AB} \sigma_{AB}$ and $\sigma_A^{deloc.}$.

Both the terms σ_{AB} and $\sigma_A^{deloc.}$ are due to electron circulations external to the nucleus A. The contribution σ_{AB} arises from induced currents on the neighbouring atom B. The nature of the induced field generated by these currents is such that a theoretical calculation of this term is based upon the anisotropy of the susceptibility tensor of the neighbouring atom.

If a molecule has delocalized electrons, there is the possibility of electron circulations of much larger radius than that of local circulations. The contribution of the delocalized electrons to the shielding constant is usually large. A notable example of a

delocalized circulation is the Larmor precession of the $p\pi$ electrons of benzene in an external field H^{o}. This precession in the case of an aromatic ring compound is commonly called the ring current.

B - THE EFFECT OF ANISOTROPY ON THE SHIELDING CONSTANT

The physical properties of a single molecule in general depend on the direction along which they are measured relative to the molecular axes; this phenomenon is called anisotropy. The reason for the anisotropy lies in the pattern of the atoms. Along any direction through a molecule or any other arrangement of atoms, the atoms occur at different intervals and different angles than they do along another direction; also, the atoms in general do not lie symmetrically about the direction. Any physical property dependent on the pattern of the atoms will vary with this direction. Thus in defining the magnetic field $\underline{H}'$ induced by an applied field $\underline{H}^o$, assumption of a linear relationship between cause and effect does not require the magnitude of $\underline{H}'$ to be independent of direction, nor the vector $\underline{H}'$ to be parallel to the vector $\underline{H}^o$. In general the induced field will not have the same direction as the applied field, and relative to an arbitrary system of Cartesian coordinates, the components of the induced field may be written

$$(37) \qquad H'_x = (\chi_{xx}H^o_x + \chi_{xy}H^o_y + \chi_{xz}H^o_z)$$

$$(38) \qquad H'_y = (\chi_{yx}H^o_x + \chi_{yy}H^o_y + \chi_{yz}H^o_z)$$

$$(39) \qquad H'_z = (\chi_{zx}H^o_x + \chi_{zy}H^o_y + \chi_{zz}H^o_z)$$

where χ_{xy} is the field induced along the x axis by unit field applied along the y axis. The terms χ_{ij} compose the susceptibility tensor

$$\begin{bmatrix} \chi_{xx} & \chi_{xy} & \chi_{xz} \\ \chi_{yx} & \chi_{yy} & \chi_{yz} \\ \chi_{zx} & \chi_{zy} & \chi_{zz} \end{bmatrix}$$

which is a second rank tensor. (9)

Onsager (10, 11) has shown that this tensor is symmetric, and it can be shown that a symmetric second order tensor has principal axes (12). By referring the tensor to its principal axes, a much simpler form is obtained,

$$\begin{bmatrix} \chi_1 & 0 & 0 \\ 0 & \chi_2 & 0 \\ 0 & 0 & \chi_3 \end{bmatrix}$$

giving $H'_x = \chi_1 H^o_x$; $H'_y = \chi_2 H^o_y$; $H'_z = \chi_3 H^o_z$. The anisotropy of such a system is observed in the fact that in general $\chi_2 \neq \chi_1$ and $\chi_3 \neq \chi_1$; $\chi_3 \neq \chi_2$.

In macroscopic measurements made on liquids and gases this anisotropy, which is a property of single molecules, disappears in an averaging process. Thus the bulk diamagnetic susceptibility would be

$$\chi_{bulk} = 1/3\ (\chi_1 + \chi_2 + \chi_3). \tag{40}$$

Annuclear magnetic resonance measurement does not represent

a measure of bulk diamagnetic susceptibility, but rather reflects the effect of the induced diamagnetic field of a molecule on one of its nuclei. The simplest way to approximate the effect of the induced molecular diamagnetic field is to assume the field to be generated by a number of point magnetic dipoles (13, 14). The value of the magnitude of each dipole, and the effect its magnetic field has on one nucleus of the molecule depends on the orientation of the molecule. The value observed in a nuclear magnetic resonance spectrum, however, involves an average over all orientations. A simple way to find this average effect is to consider the effect along the three principal susceptibilities at the nucleus under consideration and take the mean. In the simplest case in which one of the principal axes lies along the line joining the nucleus under consideration with the point dipole, the situation is as shown in the diagrams of Figure 8.

When principal axes 1 (Figure 8a) lies along the applied field the magnitude of the point dipole is taken as $\chi_1 \underline{H}^o$ and the induced magnetic field is seen to decrease the field observed at the nucleus. The contribution to the shielding constant for the nucleus is (13)

$$(41) \quad -\Delta\sigma_1(//) = \frac{2}{R^3} \chi^1_{\text{atomic}}$$

where R is the distance between the nucleus and point dipole.

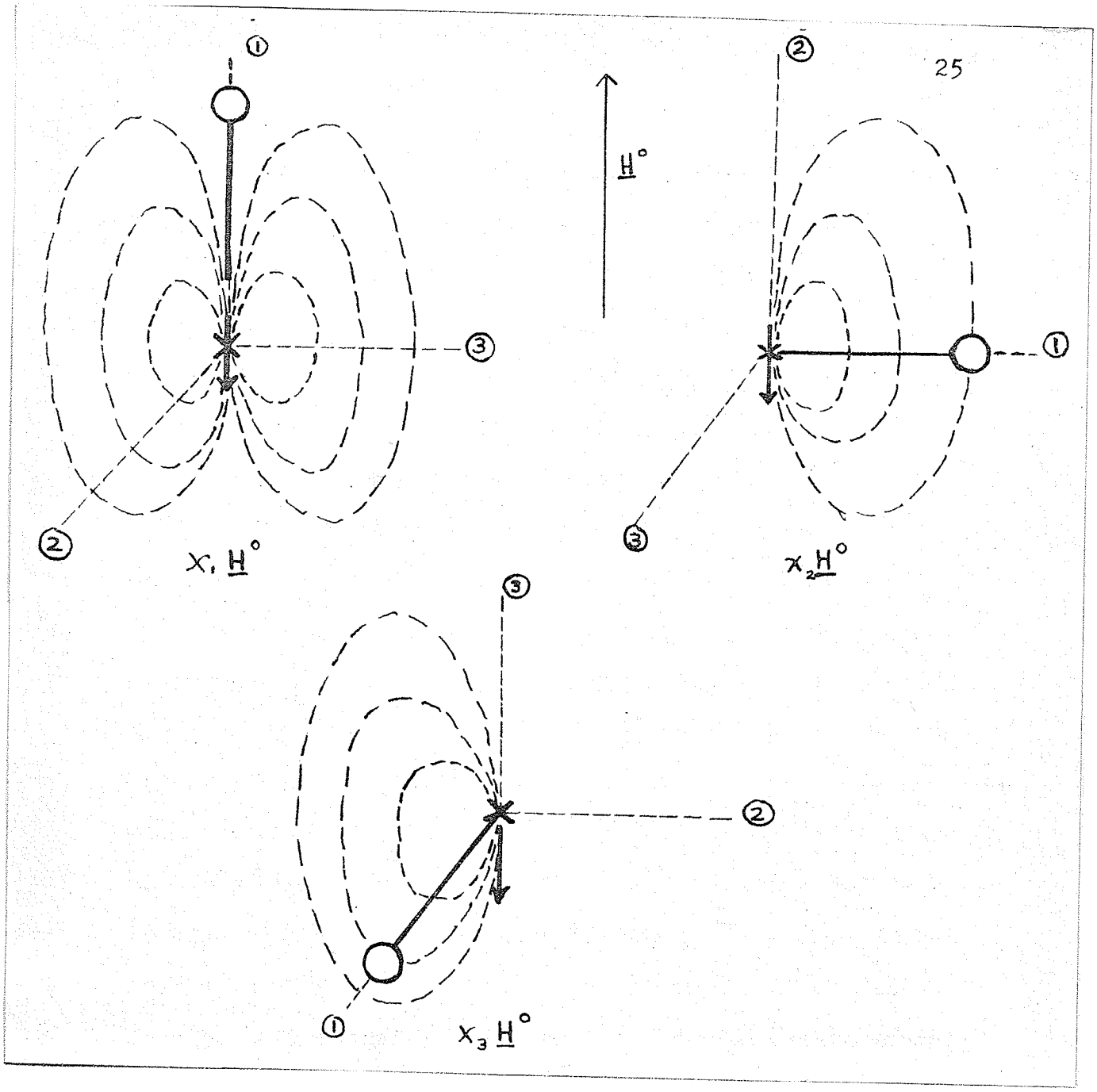

Figure 8: Effect of the field due to a neighbouring point dipole.

When the principal axis 2 (Figure 8b) lies along the applied field $\underline{H}^{o}$, the magnitude of the point dipole is $\chi_{2}\underline{H}^{o}$ and the effect is to increase the field observed

at the nucleus, that is,

$$(42) \qquad \Delta\sigma_2(\perp) = + \frac{1}{R^3} \chi^2_{\text{atomic}}.$$

When the principal axis 3 (Figure 8c) lies along the applied axis

$$(43) \qquad \Delta\sigma_3(\perp) = + \frac{1}{R^3} \chi^3_{\text{atomic}}.$$

It is seen that on averaging over all orientations of the molecule, the induced diamagnetic field of the molecule alters the shielding constant by

$$(44) \qquad \Delta\sigma = \frac{-1}{3R^3} (2\chi^1_{at} - \chi^2_{at} - \chi^3_{at}).$$

Equation (44) may be generalized to the case in which the line joining the point dipole and the nucleus does not lie along the principal susceptibility. After introducing the angular dependence of the field of the point dipole

$$(45) \qquad \Delta\sigma = \frac{1}{3R^3}\left\{\chi^1_{at}(1 - 3\cos^2\gamma_1) + \chi^2_{at}(1 - 3\cos^2\gamma_2) + \chi^3_{at}(1 - 3\cos^2\gamma_2)\right\}$$

where γ_1, γ_2, and γ_3 are the angles between the connecting line and the respective principal axes.

The value of $\Delta\sigma$ is very simply obtained for certain molecules. In the special case where $\chi_1 = \chi_2 = \chi_3$ and the molecule is isotropic there is no alteration of the shielding constant by diamagnetic fields induced in the molecule. In the additional special case in which

$\chi_1 = \chi_2 + \chi_3$ there is also no alteration of the shielding constant. In the general case, however, the molecular anisotropy shows up as a change in the shielding coefficient.

C - INTERATOMIC CURRENTS

1. Development of the Ring Current Theory

Benzene and other aromatic hydrocarbons are characterized by a π electron system which is not localized. The abnormally large diamagnetic anisotropy of such aromatic molecules has come to be explained as arising from the Larmor precession of electrons in orbits including many nuclei (15). Pauling (16) developed this idea into an approximate quantitative treatment of the diamagnetic anisotropy of crystalline benzene. For the cylindrically symmetrical case, the contribution of an electron to the magnetic susceptibility is given by the Pauli expression

$$(46) \qquad \chi = -\frac{Ne^2}{4mc^2}(\rho^2)_{av.}$$

where N = Avogadro's number and $(\rho^2)_{av.}$ = mean square of the distance of the electron from the cylindrical axis. Substitution of the distance from the axis to the carbon nucleus (1.39 A^0) for ρ gave a predicted value for the anisotropy of benzene of -49.2×10^{-6} which compared favourably with an experimental value of -54×10^{-6} (17).

The diamagnetic anisotropy of aromatic rings is observed in nuclear magnetic resonance spectra in the internal chemical shift between a hydrogen in an aromatic system and a hydrogen in an ethylenic system. The only

difference in environment for the two hydrogens is the interatomic currents. Pople (18) obtained an estimation of the shift utilizing a classical model in which the $\tilde{\pi}$ electrons are considered to move in a circular path in the plane of the ring of carbon atoms. In the presence of a magnetic field $\underline{H}^{o}$ perpendicular to the plane of the ring the $\tilde{\pi}$ electrons precess with the frequency

$$(47) \qquad \underline{\omega} = \frac{e\underline{H}^{o}}{2mc}$$

producing a current per electron equal to

$$(48) \qquad i = \frac{e\,\underline{\omega}}{2\tilde{\pi}} .$$

For a system containing six electrons this gives rise to an interatomic current

$$(49) \qquad I = \frac{3e^{2}H^{o}}{2\tilde{\pi}mc} .$$

Pople replaced the circular magnetic shell produced by such a current by an approximately equivalent magnetic dipole located at the center of the ring of magnitude

$$(50) \qquad \mu = \frac{3e^{2}H^{o}a^{2}}{2mc^{2}}$$

where a = radius of circle and is taken to be C-C bond distance. The dipole lies parallel to and opposed to the applied field. The field produced is thus opposed to the applied field at the center ofthe ring but re-inforces it at the position of the hydrogen atom (Figure 9).

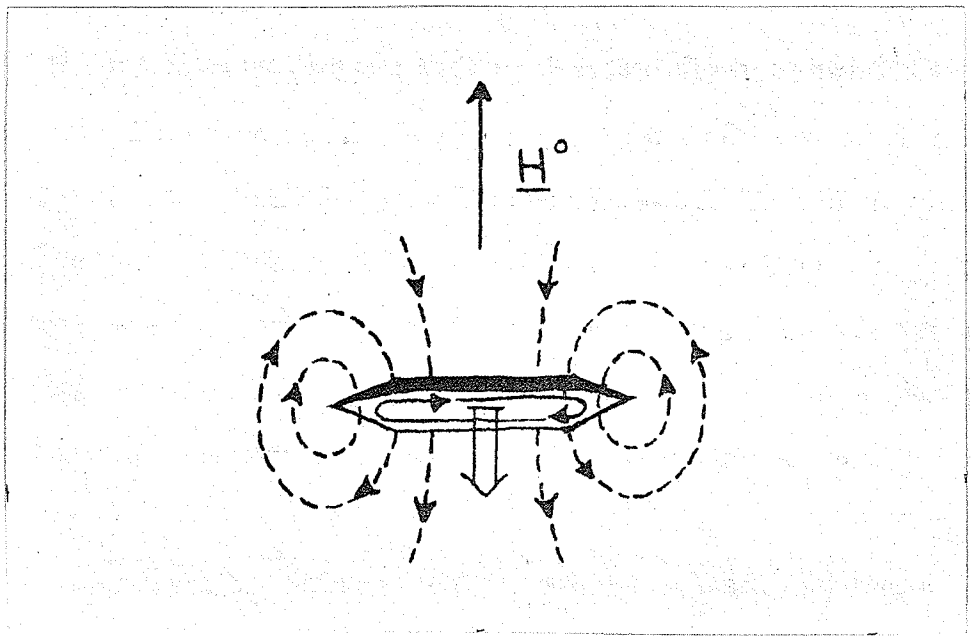

Figure 9: Magnetic field produced by ring current.

The effect of the interatomic ring current therefore is to produce a chemical shift of the aromatic proton to low field. The magnitude of the magnetic field at the hydrogen atom due to the ring current is

$$H' = \frac{3e^2H^oa^2}{2mc^2(a+b)^3} \qquad (51)$$

where a = C-C interatomic distance and b = C-H interatomic distance. This represents the magnetic field induced by an applied field perpendicular to the plane of the ring. For comparison with nuclear magnetic resonance measurements the average over all orientations is required. Due to the symmetry of the benzene molecule this average may be obtained by the summation process

$$(52) \qquad H'_{av} = 1/3\ (H'_{\perp} + 2H'_{//})$$

where $H'_{\perp}$ is the field induced by $\underline{H}^{o}$ perpendicular to the ring and $H'_{//}$ is the field induced by $\underline{H}^{o}$ parallel to the ring. Since no ring current is induced by a field applied parallel to the ring, $H'_{//}$ is zero and

$$(53) \qquad H'_{av} = 1/3\ (H'_{\perp}) = \frac{e^2Ha^2}{2mc^2(a+b)^3} .$$

Therefore, the internal chemical shift between the aromatic hydrogen and the ethylenic hydrogen should be

$$(54) \qquad \delta = \frac{H'}{H^{o}} = \frac{e^2a^2}{2mc^2(a+b)^3}$$

The calculations of Pople were refined by Waugh and Fessenden (19). This treatment still employs a classical basis but the magnetic field is calculated without making the magnetic dipole approximation. In cylindrical polar coordinates, the value of the magnetic field induced by a field applied perpendicular to the plane of the ring is

$$(55) \qquad H' = \frac{3e^2H^{o}}{2\pi mca} \cdot \frac{2}{\left[(1+\rho)^2 + z^2\right]^{\frac{1}{2}}}\left[K + \frac{1-\rho^2-z^2}{(1-\rho)^2+z^2} E\right]$$

where ρ, z are cylindrical polar coordinates for the ring and K, E are elliptic integrals. On averaging over all orientations the value for $\langle H' \rangle_{av}$ obtained by Waugh and Fessenden (19) was

$$(56) \qquad \langle H' \rangle_{av} = \frac{e^2H^{o}}{4\pi mc^2a} \frac{1}{2\pi\rho^{\frac{1}{2}}}\left[K(k) + \frac{1-\rho^2-z^2}{(1-\rho)^2+z^2} \cdot E(k)\right]$$

which was subsequently corrected by Waugh (20) to

$$(57) \qquad \langle H' \rangle_{av} = \frac{e^2 H^o}{4\pi mc^2 a} \frac{\pi \rho^{\frac{1}{2}}}{2} \left[K(k) + \frac{1 - \rho^2 - z^2}{(1 - \rho)^2 + z^2} E(k) \right]$$

and

$$(58) \qquad \delta = \frac{\langle H' \rangle_{av}}{H^o}$$

Assuming a diamagnetic ring current in the plane of the ring Waugh and Fessenden (19, 20) found a predicted value for δ which was too high. The π electron cloud is assumed to exist as two doughnut shaped rings lying above and below the plane of the carbon atoms. Assuming a separation between the rings of about 1.2 A^o the predicted and experimental values for δ of benzene were brought into agreement.

Johnson and Bovey (21) carried out calculations using equation (59) which they attributed to Waugh and Fessenden's correction.

$$(59) \qquad \langle H' \rangle_{av} = \frac{e^2 H^o}{\pi mc^2 a} \frac{1}{\left[(1 + \rho)^2 + z^2\right]^{\frac{1}{2}}} \left[K + \frac{1 - \rho^2 - z^2}{(1 - \rho)^2 + z^2} E \right]$$

The most probable value for δ was chosen from experimental values for the shift between the benzene proton and the ethylenic proton in such substances as cyclooctatriene - 1,3,5, and cyclooctatetraene. This value when substituted in the Waugh equation for δ yielded a value for the separation of the two rings of current of 1.28 A^o. Using this empirically chosen value for the separation of the two ring currents,

and evaluating the elliptic integrals by computer, Johnson and Bovey (21) produced tables showing the value of δ for unit increments of ρ and z between 0.00 and 4.00 in increments of 0.01 where the units are ring radii (which is equal the C-C bond distance 1.39 A^{o}).

Following Pauling's (16) semi-classical treatment of the anisotropy of benzene, London (22) carried out a quantum mechanical calculation to determine the molecular orbitals of π electrons and the associated molecular magnetic moment in a conjugated hydrocarbon in the presence of a uniform external magnetic field. The London theory is based on the simple L. C. A. O. theory of Hückel, that, is the molecular orbital ψ_i is written as the sum of atomic orbitals ϕ_s, $\psi_i = \sum_s c_s \phi_s$, and the coefficients c_s are determined by a variational procedure. London modified the theory by modifying the atomic orbitals ϕ_s so as to eliminate difficulties arising from choice of origin. Pople (23) extended the method of London from the case of a uniform external field to a nonuniform field. This permitted a calculation of the ring currents in polycyclic compounds relative the ring current in benzene. The chemical shift for a ring proton relative to benzene may be calculated from these values.

2. Application of the Ring Current Theory

In a paper by Bernstein, Schneider and Pople (24) application of the ring current theory was made to a series of polycyclic aromatic hydrocarbons. Assuming the current flowing in each hexagon equal to that in benzene, the effect of this current was found from the point dipole approximation of Pople (18). The theoretically predicted values reproduced trends observed in experimental data, but absolute agreement was unsatisfactory. In another approach, Jonathon, Gordon and Dailey (25) determined the current intensity in each ring of the polycyclic compound employing the molecular orbital method of Pople (23). Chemical shifts relative to benzene were calculated from the tables of Johnson and Bovey (21). However, these calculated shifts are substantially larger than the experimentally measured shifts. A comparison of calculated and experimental results reveals a linear equation relating the two sets of chemical shifts (Figure 10).

$$(60) \qquad \Delta\sigma_{(exp'l)} = 0.63\ \Delta\sigma_{(calc'd)} - 0.13$$

where $\Delta\sigma$ = the portion of the chemical shift due to anisotropy effects.

The implications behind this relation are rather more than empirical. The early theories of the diamagnetic anisotropy of benzene were based upon the assumption that the anisotropy was due solely to the $p\pi$ electrons involved

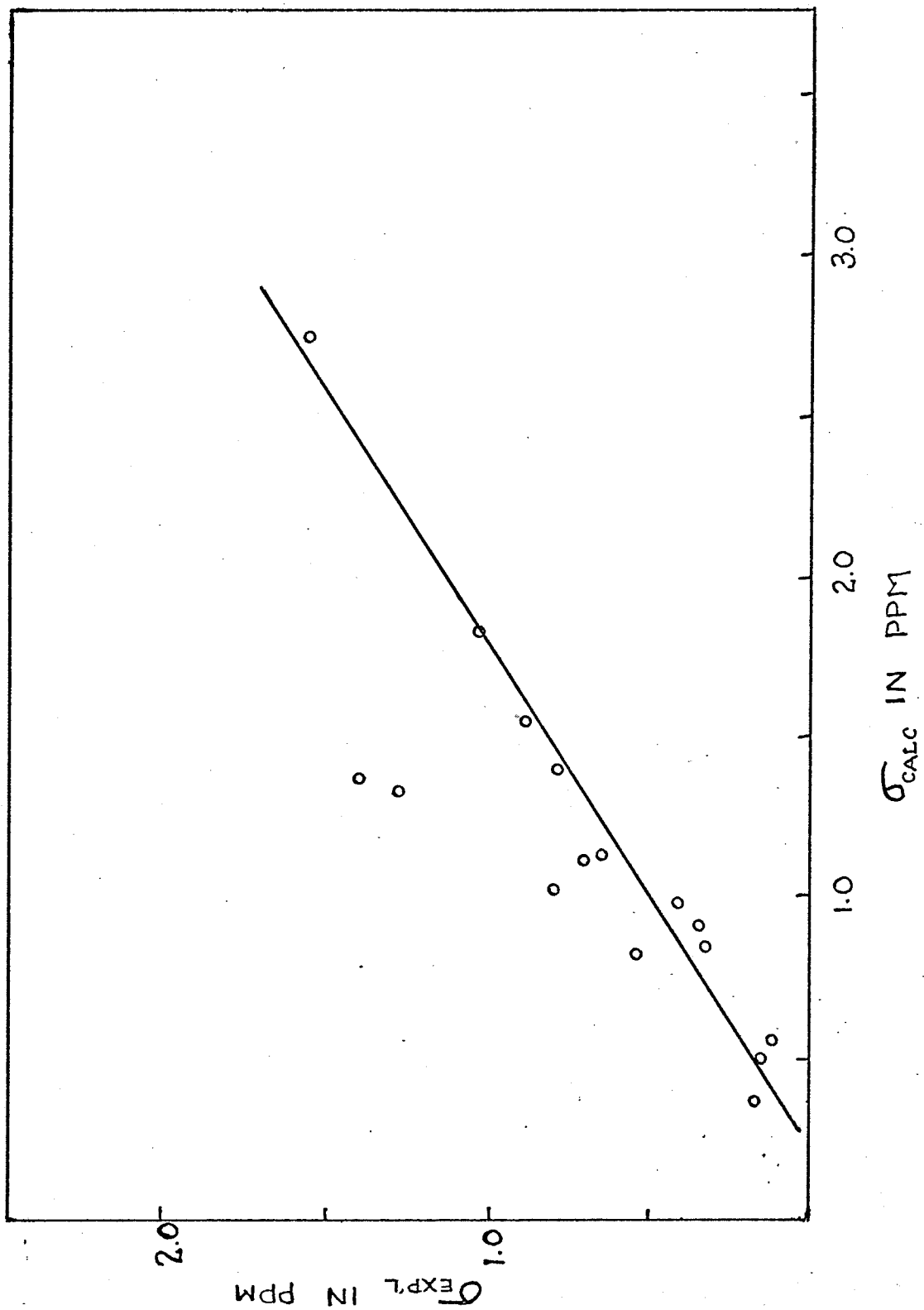
2.0
1.0
σ_{EXPL} IN PPM
1.0
2.0
3.0
σ_{CALC} IN PPM

in the ring current . More recent work (26, 27), however, has employed the molecular orbital theory of the aromatic ring to show that a significant contribution to the anisotropy is due to localized p $\tilde{\pi}$ electrons. Thus Pople (27) states that the diamagnetic susceptibility χ is given by

(61) $$\chi = \chi_{ring} + (\chi_d^{at} + \chi_p^{at})$$

where χ_d^{at} = local diamagnetic susceptibility and χ_p^{at} = local paramagnetic susceptibility and the paramagnetic term accounts for most of the anisotropy due to local circulations of electrons. An approximate calculation of this paramagnetic anisotropy term, $\Delta\chi_p$, by Pople (27) indicates that it contributes about 30% of the total anisotropy. In the same paper he makes an order of magnitude calculation of $\Delta\sigma_{local}$, the chemical shift of benzene due to local circulations.

(62) $$\Delta\sigma_{local} = \Delta\chi_{local}/3R^3N$$

In order to obtain a comparison with experimental results, Pople calculated the difference between $\Delta\sigma_{local}$ for benzene and ethylene

(63) $$\Delta\sigma_{local \text{ for benzene}} - \Delta\sigma_{local \text{ for ethylene}} = -0.7 \text{ p.p.m.}$$

(N.B. approximate calculation only). This value is compared with the chemical shift difference observed between the benzene hydrogen and ethylenic hydrogen:

(64) $$\sigma_{\text{benzene H}} - \sigma_{\text{ethylene H}} = -1.5 \text{ p.p.m.}$$

The result indicates that local circulation comprises a significant proportion of the $\Delta\sigma$, the part of the chemical shift due to anisotropy effects. Clearly, by neglecting the anisotropy arising from local circulation of p π electrons, Waugh and Fessenden (19) have attributed too large a chemical shift to the ring current anisotropy.

Subsequent calculations made by Johnson and Bovey (21) employ the experimental value of -1.5 p.p.m. (equation 64) to evaluate the parameter representing the separation of the two ring currents in Waugh and Fessenden's equation. Such an evaluation will lead to an exaggerated value of the parameter. Calculations carried out on polycyclic aromatic hydrocarbons, then, will yield a value of $\Delta\sigma$ which is too large.

Chapter III

THE COUPLING CONSTANT

A - THE THEORY OF THE COUPLING CONSTANT

The theory of nuclear coupling is developed in a number of reference works, (28, 29, 30). A magnetic field applied to a molecule causes a motion of the electrons which contributes to the magnetic field at a nucleus of the molecule. In addition to the chemical shift, the presence of a magnetic dipole on a neighbouring nucleus can contribute to the magnetic field at the nucleus under observation. This latter effect is known as coupling. The coupling between two nuclei, A and B, with magnetic moments $\boldsymbol{\mu}_A$ and $\boldsymbol{\mu}_B$ is expressed by:

$$\text{Coupling} \propto \boldsymbol{\mu}_A \cdot \boldsymbol{\mu}_B$$

$$= J_{AB} \boldsymbol{\mu}_A \cdot \boldsymbol{\mu}_B$$

the proportionality constant J_{AB} being termed the coupling constant.

In the case of a solid crystalline lattice held fixed in orientation with respect to the magnetic field, it is easy to understand how coupling exists. Thus given two nuclei A and B with nucleus A under observation, the magnetic moment assigned to nucleus B generates a magnetic field according to the classical rules of magnetostatics (Figure 11). The resulting magnetic field observed at B is determined by simple geometrical factors.

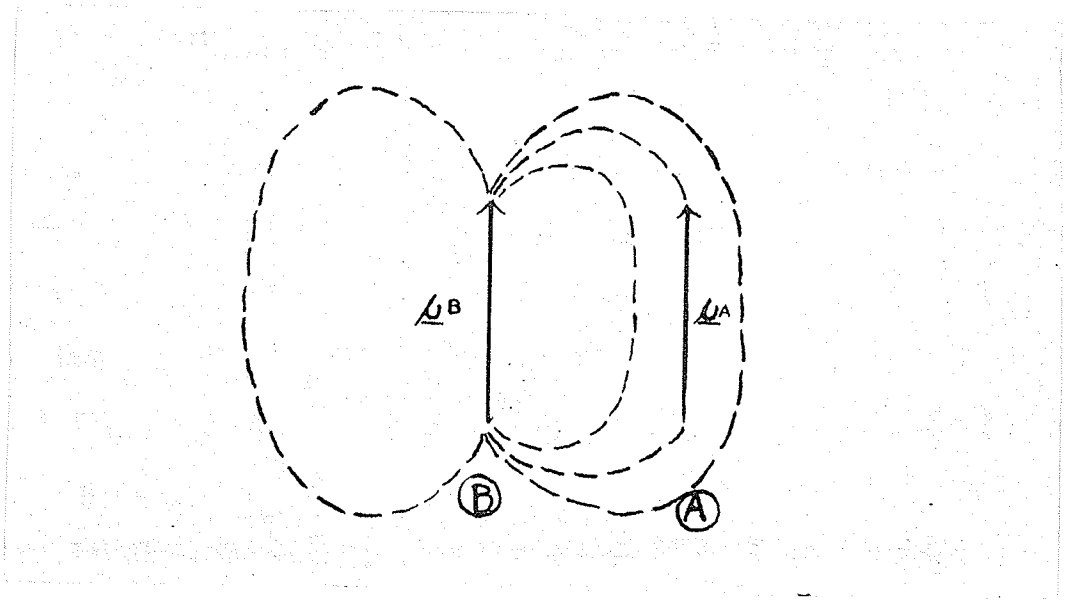

Figure 11: Coupling in a crystalline lattice.

When the nuclear magnetic resonance spectrum is taken of liquid or gaseous samples such simple geometrical interactions are destroyed by averaging processes. In this case another interaction of smaller magnitude becomes significant. The basis of this interaction may be illustrated on an approximate physical basis by considering the valence bond model for the molecule (Figure 12). In a diatomic molecule of nuclei A and X with two bonding electrons, electron (a) "belongs" to nucleus A and electron (x) "belongs" to nucleus X. In the case that nucleus X has orientation with magnetic moment down the more stable configuration for electron (x) is that with spin up. The theories of chemical bonding require that the electrons in

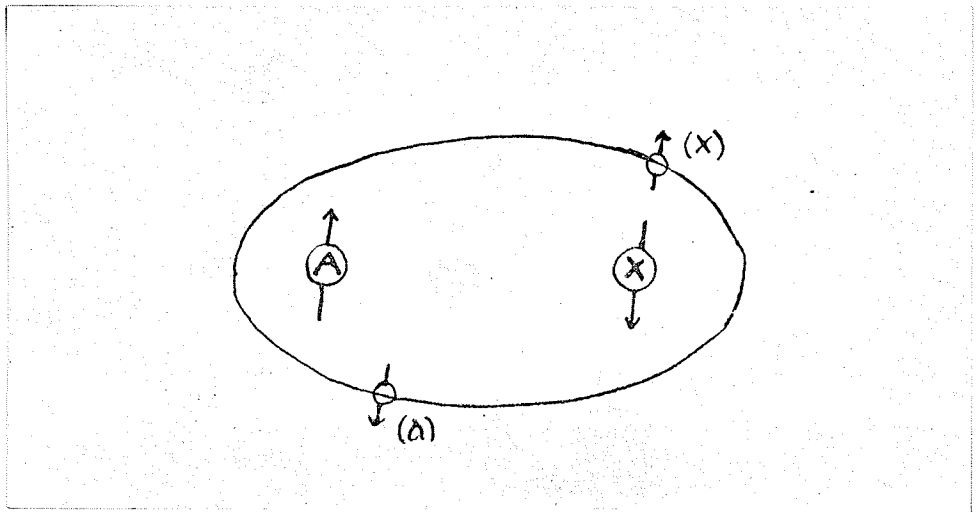

Figure 12: Coupling in the liquid or gaseous phase.

the same bonding orbital have spins opposed. Thus the most stable state is that in which the nucleus-electon-electron-nucleus spins alternate as shown in the figure above, (Figure 12). The spins of nuclei A and X are preferentially paired and the coupling is defined as positive.

B - COUPLING CONSTANT IN THE AROMATIC RING

The values of the coupling constants between the ring hydrogen nuclei in substituted benzenes have been found to lie in the ranges $J_{HH'}^{ortho}$ = 6 to 9 cycles/sec., $J_{HH'}^{meta}$ = 1 to 3 cycles/sec. and $J_{HH'}^{para}$ = 0 to 1 cycles/sec.(30) Coupling is determined by both σ and π bond mechanisms and $J_{HH'}$ may be written as

$$J_{HH'} = J_{HH'}(\sigma) + J_{HH'}(\pi). \tag{65}$$

Of the two terms in equation (65) the magnitude of $J_{HH'}(\sigma)$ decreases rapidly as the number of bonds separating the two nuclei increases. Values for the second term, $J_{HH'}(\pi)$, have been calculated by McConnell (31, 32) for aromatic hydrocarbons on the basis of a σ-π exchange polarization mechanism. The results of these calculations combined with the expected values of $J_{HH'}(\sigma)$ indicates that the main coupling mechanism for ortho and meta hydrogen is via σ bonds. $J_{HH'}^{para}(\sigma)$, however, is almost certainly negligible and the π bond mechanism dominates the para coupling.

The analysis of the proton system for aromatic hydrocarbons gives the magnitude of the coupling constant, but not the absolute sign. Buckingham and McLauchlan (33) studied the spectrum of p-nitrotoluene in the presence of an electric field applied parallel the main field. The

results indicated that the ortho ring coupling is positive. Positive ortho coupling has also been found by Saupe and Englert (34) and by Snyder and Anderson (35).

The absolute sign of meta and para couplings is determined from information concerning the signs relative to ortho couplings. Martin and Dailey (36) determined that the meta and para coupling constants have the same relative sign as the ortho coupling for a group of approximately twenty-five para-disubstituted benzenes. On the basis of a positive value for the ortho coupling constant between ring protons, the meta and para couplings are assigned positive values. This result is supported by work carried out by Banwell, Cohen, Sheppard and Turner (37), Grant, Hirst and Gutowsky (38), Cox (39) and Freeman, Bhacca and Reilly (40). There is no known evidence to indicate the existence of a negative coupling constant between the ring protons of an aromatic hydrocarbon.

Chapter IV

ANALYSIS OF THE AA'BB' SPECTRUM

ANALYSIS OF THE AA'BB' SPECTRUM

The calculation of an energy diagram for the spin states of the nucleus is a preliminary to the analysis of the nuclear magnetic resonance spectrum. In the particular case of a single uncoupled proton the energy diagram can be readily calculated from the classical model of the spin states +1/2 and -1/2. Calculations carried out on complex systems are done quantum mechanically.

The proton has two spin states, +1/2 and -1/2, represented respectively by the wave functions α and β. A molecule containing n protons has 2^n spin states which are the combinations of the two possible spin states for each proton. The spin states are written

$$\phi_i = \alpha(1)\ \beta(2)\ \alpha(3)\ \ldots\ \beta(n)$$

where the bracketed numeral designates the nucleus to which the nuclear spin function α or β refers. Such spin states are frequently written

$$\phi = \alpha\beta \ldots \beta$$

with the numerical assignment understood. The nuclear spin states constitute an orthonormal set,

$$\int \phi_i \phi_j^* \, d\tau = \delta_{ij}$$

and are used as a basis set in the formation of spin wave functions ψ_l,

$$\psi_l = c_{l1}\phi_1 + c_{l2}\phi_2 + \ldots c_{li}\phi_i + \ldots c_{ln}\phi_n$$

The energy levels are calculated from the time independent Schroedinger equation

$$\mathcal{H}\psi_l = E_l\psi_l$$

where $\mathcal{H}$ is the Hamiltonian operator for a coupled nucleus in a magnetic field and E_l is the energy of the wave function ψ_l. Solution for the energy levels is carried out by the variational procedure on the linear combinations. The coefficients c_{li} are calculated from the set of linear equations

$$\left| (H_{ij} - \delta_{ij}E)\ c_{lj} \right| = 0$$

where $H_{ij} = \int \phi_i \mathcal{H} \phi_j^* d\tau$. The set of linear equations known as the secular equations, have a nontrivial solution only if the determinant of the coefficients of c_{lj} equals zero.

$$\left| H_{ij} - \delta_{ij}E = 0 \right|$$

or after expansion

$$\begin{vmatrix} H_{11} - E & H_{12} & H_{13} & \cdot & \cdot \\ H_{21} & H_{22} - E & H_{23} & \cdot & \cdot \\ H_{31} & H_{32} & H_{33} - E & \cdot & \cdot \\ \cdot & \cdot & \cdot & \cdot & \cdot \\ \cdot & \cdot & \cdot & \cdot & \cdot \end{vmatrix} = 0$$

The simplest application of the method is to the evaluation of energy levels for an AB system, consisting by definition of two nuclei; for a description of the

nomenclature used to classify the systems of magnetic nuclei see reference (41). There are $2^2 = 4$ basis spin functions, $\alpha\alpha$, $\alpha\beta$, $\beta\alpha$, $\beta\beta$, and the secular equations yield a 4 x 4 determinant

$$\begin{vmatrix} H_{11} - E & H_{12} & H_{13} & H_{14} \\ H_{12} & H_{22} - E & H_{23} & H_{24} \\ H_{13} & H_{23} & H_{33} - E & H_{34} \\ H_{14} & H_{24} & H_{34} & H_{44} - E \end{vmatrix} = 0$$

The nature of the AB system is such that all off-diagonal elements but H_{23} are zero. The determinant breaks down into one 2 x 2 determinant and two 1 x 1 determinants and the energy levels may be determined analytically.

An AB_2 nuclear system has $2^3 = 8$ basis spin functions, and the secular equations produce an 8 x 8 determinant. Symmetry conditions and the nature of the system break the determinant down into four 1 x 1 determinants and two 2 x 2 determinants. Again the energy levels may be obtained analytically. With increasing numbers of nuclei the spin systems become more complex, the solution of the secular equation more difficult, the number of energy levels greater and the assignment of transitions to lines in the spectrum less certain. The determinant for the ABC system factorizes into two 1 x 1 determinants and two 3 x 3 determinants. The 3 x 3

determinant cannot be solved analytically, and approximation methods are used.

The AA'BB' system generates a 16 x 16 determinant which factorizes into two 1 x 1, five 2 x 2, and one 4 x 4 sub-determinant . All may be solved analytically but the 4 x 4 determinant, and explicit values can be given for only twelve of the sixteen energy levels. Application of selection rules to the AA'BB' system predicts a symmetrical theoretical spectrum of twenty-eight lines of which four are weak intensity combination transitions and are neglected. Of the remaining twenty-four lines only one of the symmetrical halves is treated. The transition energies, and intensities corresponding to the twelve lines are summarized in Table I using the notation of Dischler and Maier (42).

The parameters K, L, M, N and C, D, F, G of Table I are defined in terms of the coupling constants and the chemical shift.

$$N = J_{13} + J_{14} \tag{66a}$$

$$L = (J_{13} - J_{14}) \geq 0 \tag{66b}$$

$$K = (J_{12} + J_{34}) \geq 0 \tag{66c}$$

$$M = (J_{12} - J_{34}) \geq 0 \tag{66d}$$

where the J's are the coupling constants defined in Figure 13.

Table I

SUMMARY OF TRANSITIONS AND INTENSITIES

Line		Transitions	Energies relative to center (c/s)	Intensities *
a	1†	$1S_1' \rightarrow S_2$	$(C + N)/2$	$1 - N/C$
b	3	$S_{-2} \rightarrow 1S_{-1}'$	$(C - N)/2$	$1 + N/C$
c	9	$2a_0 \rightarrow 2a_1'$	$(D + G)/2$	$\sin^2(\Theta - \psi)$
d	10	$2a_{-1} \rightarrow 1a_0'$	$(F + G)/2$	$\cos^2(\Theta + \chi)$
e	11	$1a_0 \rightarrow 2a_1'$	$(D - G)/2$	$\cos^2(\Theta - \psi)$
f	12	$2a_{-1} \rightarrow 2a_0'$	$(F - G)/2$	$\sin^2(\Theta + \chi)$
g	7	$4S_0 \rightarrow 2S_1'$	$\frac{1}{2}C + \frac{1}{4}K - \Omega_3$	$\left[(a_{31} + a_{32})\cos\Phi + (a_{32} + a_{34})\sin\Phi\right]^2$
h	8	$2S_{-1}' \rightarrow 3S_0'$	$\frac{1}{2}C - \frac{1}{4}K + \Omega_2$	$\left[(a_{22} + a_{24})\cos\Phi - (a_{21} + a_{22})\sin\Phi\right]^2$
i	5	$3S_0' \rightarrow 2S_1'$	$\frac{1}{2}C + \frac{1}{4}K - \Omega_2$	$\left[(a_{21} + a_{22})\cos\Phi + (a_{22} + a_{24})\sin\Phi\right]^2$
j	6	$2S_{-1}' \rightarrow 4S_0'$	$\frac{1}{2}C - \frac{1}{4}K + \Omega_3$	$\left[(a_{32} + a_{34})\cos\Phi - (a_{31} + a_{32})\sin\Phi\right]^2$
k	2	$1S_0' \rightarrow 1S_1'$	$-\frac{1}{2}C + \frac{1}{4}K - \Omega_4$	$\left[(a_{43} + a_{44})\cos\Phi - (a_{41} + a_{42})\sin\Phi\right]^2$
l	4	$1S_{-1}' \rightarrow 2S_0'$	$-\frac{1}{2}C - \frac{1}{4}K + \Omega_1$	$\left[(a_{11} + a_{12})\cos\Phi + (a_{12} + a_{14})\sin\Phi\right]^2$

*The total sum of the intensity of the half-spectrum is 8.
†The numbers are the labels used by Pople (43).

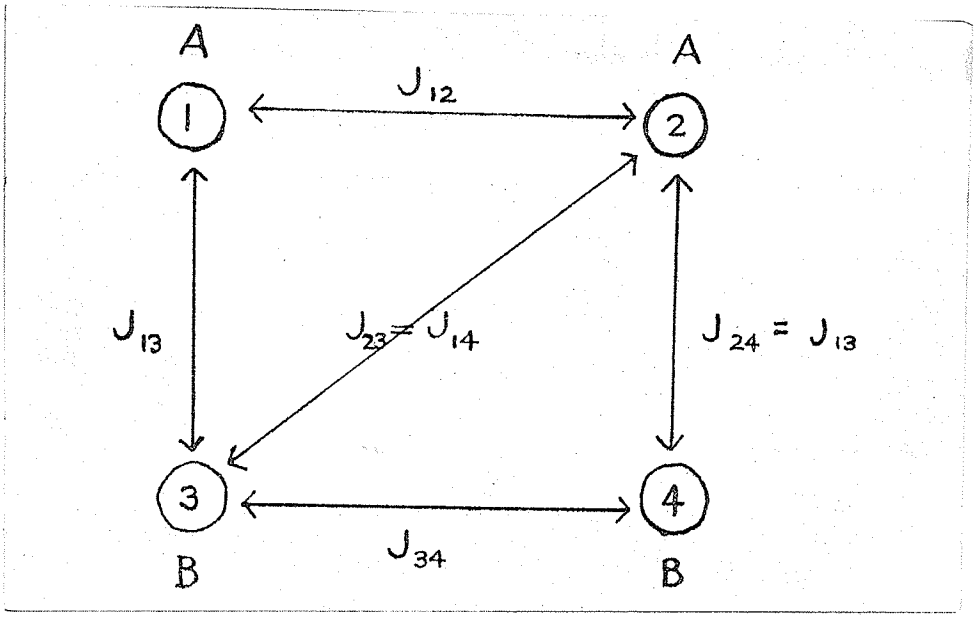

Figure 13: Coupling for an AA'BB' system.

$$(67a) \qquad C = \sqrt{(\nu_o \delta)^2 + N^2}$$

$$(67b) \qquad D = \sqrt{(\nu_o \delta + M)^2 + L^2}$$

$$(67c) \qquad F = \sqrt{(\nu_o \delta - M)^2 + L^2}$$

$$(67d) \qquad G = \sqrt{M^2 + L^2}$$

where $\nu_o \delta$ is the chemical shift in cycles/second. The quantities $\sin\theta$, $\sin\psi$, $\sin\chi$ and $\sin\Phi$ are defined in terms of the above parameters. The Ω's which occur in transitions "g" to "l" are the eigenvalues of the 4 x 4 submatrix, and the a_{ik}'s are the corresponding eigenvectors.

The transitions "a" to "f" are sufficient to determine the chemical shift $\nu_o \delta$ and the parameters

L, M and N. Inspection of Table I indicates that the transition energies for lines "a" to "f" do not involve the energies detained from the 4 x 4 determinant but that the 4 x 4 determinant must be solved in order to evaluate transition energies for lines "g" to "l". The parameter K is the only additional information obtained from lines "g" to "l". Pople, Schneider and Bernstein (43) in analyzing an AA'BB' spectrum avoided the difficulty of solving the 4 x 4 determinant by assuming $J_{12} \approx 0$ and K = -M. This approximate solution is applicable in cases for which J_{12} (or $J_{AA'}$) is known to be very small or zero.

Dischler and Maier (42) have evaluated all of the parameters of the AA'BB' system without assuming K = -M. Matrix theory states that the sum of the eigenvalues of the matrix is equal to the trace of the matrix. Applying this property to the 4 x 4 determinant gives

$$\Omega_1 + \Omega_2 + \Omega_3 + \Omega_4 = -N.$$

Combining this equation with the last six relations in Table I, Dischler and Maier obtained an explicit expression for K. They were thus able to list all the following relations defined for a system of twelve lines labelled "a" to "l":

(68a) $K = b + g + k - a - h - l$

(68b) $K = b + i + k - a - j - l$

(68c) $K = g + i + k - 2a - l$

(68d) $K = 2b + k - h - j - l$

(69) $C = a + b = g + j = h + i$

(70) $D = c + e$

(71) $F = d + f$

(72a) $G = (c - e) \geq 0$

(72b) $G = (d - f) \geq 0$

(73) $L = \sqrt{G^2 - M^2}$

(74) $M = 1/\sqrt{2}\,(ce - df)$

(75a) $N = a - b$

(75b) $N = \pm\sqrt{C^2 - (\sqrt{2}\,)^2}$

(76a) $\sqrt{2} = +\sqrt{4ab}$

(76b) $\sqrt{2} = +\sqrt{2(ec + df)}$.

In the papers by Dischler et al, a number of intensity correlations were derived.

(77) $I_a + I_b = 2$

(78) $I_c + I_e = 1$

(79) $I_d + I_f = 1$

(80) $I_a/I_b = b/a$

(81) $2 \geq (I_g + I_h + I_i + I_j) \geq 1$

(82) $2 \leq I_k + I_e \leq 3$

Dischler and Englert (44) also calculated several relations between line positions:

(83) $c \geq d$ *

(84) $e \geq f$ *

(85) $g \geq h$ *

(86) $i \geq j$ *

* Dischler and Englert concluded that $c \geq d \geq e \geq f$ and $g \geq h \geq i \geq j$. Lim, Taurins and Whitehead (45) pointed out that these statements were not correct in their entirety.

Dischler and Englert applied the above analysis of the AA'BB' to a number of ortho disubstituted benzenes, para disubstituted benzenes and furan type heterocycles.

Equations (77) through (86) may be employed to help assign the lines of an experimental spectrum. The method has been summarized by Lim, Taurins and Whitehead (45):

Step 1 - The first pair assigned has the highest intensity of the six pairs of lines, and will consist of b'' and l'' or a'' and k'' corresponding to N positive or negative.

Step 2 - Another intense pair of lines is then chosen and will consist of two lines not assigned to the first pair, namely a'' and k'' or b'' and l''. The intensity of this pair and the pair assigned in Step 6 is often very close. Therefore the intensity sum is of importance. The total intensity of one line from Step 1 and one line from Step 2

should equal 2, the sum of the remaining two lines being very nearly 2. Furthermore, from equation (76) it is known that this second pair of lines should be two or three pairs away from the first pair.

Step 3 - The innermost lines (those nearest to the center of the spectrum) are then assigned as lines "f" and "j"; they are generally of low intensity.

Step 4 - The outermost lines (those farthest from the center of the spectrum) are assigned as "c" and "g"; they are the least intense lines.

Step 5 - The remaining two pairs are of medium to high intensity; one pair lies between the two high intensity lines assigned in Steps 1 and 2 and possesses several possible assignments such as ("d","h") or ("d","i") for "i">"h" or "h">"i" when "e">"d", or such as ("e","h") or ("e", "i") for "i">"h" or "h">"i" when "d">"e".

Step 6 - The only remaing pair of lines will also possess several possible assignments such as ("e","h") or ("e","i") when "e"$\geq$"d" and ("d","h") or ("d","i") when "d">"e".

In the paper by Dischler and Englert (44) the assignment of the experimental spectra was made on the basis of "d"$\geq$"e" and "h"$\geq$"i". In addition the pairs ("e","i") and ("d","h") were chosen in Steps 5 and 6. Calculations were carried out for $N>0$ and $N<0$, but

Chapter V

ANISOTROPY AND C^{13}-H COUPLING CONSTANTS

ANISOTROPY AND C^{13}-H COUPLING CONSTANTS

Equation (36) expresses the shielding constant in terms of four contributions,

$$(36) \qquad \sigma_A = \sigma_{AA}^{dia} + \sigma_{AA}^{para} + \sum_{A \neq B} \sigma_{AB} + \sigma_A^{deloc} .$$

Of the four terms, the last two describe effects produced by the magnetic anisotropy of neighbouring atoms or groups. Theoretical estimates of these anisotropy effects are not sufficiently accurate to be employed in predicting values of σ_A and the chemical shift τ. In addition, experimental values of magnetic anisotropies are non-existent.

It has been observed that anisotropy, medium effects and other factors which complicate the chemical shift value have little effect on C^{13}-H coupling constants. Goldstein and Reddy (46) have found that in the absence of anisotropy and medium effects there is a linear relationship between the C^{13}-H couplings and the chemical shifts τ. Deviations from this linear relation were attributed to magnetic anisotropy and calculations were made on the basis of this assumption. $J(C^{13}\text{-H})$ was plotted against τ for a series of methyl and methylene protons (sp^3 saturated compounds) and also a series of sp^2 unsaturated compounds. The anisotropy of a number of ring structures and other groups was estimated. The anisotropies calculated for the same groups, where possible, from both series were in good agreement. The calculated value of the anisotropy of benzene,

-78 cycles/sec., compares favourably with a value calculated by Ito (47), -86 cycles/sec.

Goldstein and Reddy (46) included a short justification of the linear relation. Measurements of J_{CH} for directly bonded nuclei have shown a very close dependence of the magnitude of this coupling constant on the "s"-character of the C-H bond (48, 49, 50). This dependence is expressed by the relation

$$J_{CH} = J_o \alpha_H^2 \qquad (87a)$$

where α_H^2 is the "s"-character of the C-H orbital. J_o is a constant, and experimental results (49, 50) indicate the value of J_o is 500.

$$J_{CH} = 500 \alpha_H^2 \qquad (87b)$$

The shielding constant depends upon the first two terms of equation (36) in the absence of anisotropy effects. These two terms are sensitive to the hybridization of the hydrogen atom. Thus in the absence of magnetic anisotropy, or in the presence of a constant or linearly varying anisotropy, a linear relation is expected and observed between the coupling constant J_{CH} and the chemical shift τ, since both then depend on "s"-character.

Grant and Litchman (51) made a critical evaluation of the correlation of C^{13}-H coupling constants

with "s"-character. Karplus and Grant (52) determined, on a theoretical basis, the factors upon which the C-H coupling depends. Grant and Litchman showed that changes in the effective nuclear charge of the C atom can account for much of the change in C-H couplings. This change in the factor governed by nuclear charge was not considered in correlations with "s"-character (48, 49, 50).

The work by Grant and Litchman makes uncertain the correlation of C^{13}-H couplings solely with "s"-character. Many of the conclusions made assuming this correlation are likewise rendered uncertain. The linear correlation between C^{13}-H couplings and τ, however, remains an empirical fact. Application of the method of Goldstein and Reddy (46), particularly to a series of C^{13}-H couplings in which the effective nuclear charge on C^{13} changes little, can possibly yield an approximate value for the anisotropy.

The manner in which the anisotropy is obtained from the experimental data is best illustrated by considering one case from the paper by Goldstein and Reddy (46). A plot of J_{CH} vs. τ for a series of ethylenes (ethylene, vinyl chloride - cis and trans, vinylidene chloride, dichloroethylene - cis and trans, trichloroethylene, and vinylene carbonate) produces a straight line. On the same graph the position for the

C^{13}-H coupling constant of benzene lies off the line to low field. The vertical distance on the τ scale between the benzene position and the straight line is taken to be due to the difference in anisotropy for the two protons. In this case the anisotropy was attributed to the ring current.

Chapter VI

THE NATURE OF THE PROBLEM

THE NATURE OF THE PROBLEM

Triptycene is an aromatic compound composed of three benzene rings each joined to a pair of saturated bridgehead carbons from ortho positions on the benzene ring (Figure14). The object of this research is to obtain and analyze the spectrum of the triptycene molecule (an AA'BB' system) and to apply the ring current theory to the problem in an attempt to predict the chemical shifts and, subsequently, to evaluate the usefulness of the ring current model applied to a complex system.

A molecular orbital calculation after the method of Cotton (53) shows that any alteration of electron densities on the benzene rings due to overlap is entirely negligible. The molecular orbital calculation to determine the current in each ring (23) is unnecessary and the ring current is simply taken to be equal to that of benzene. The effect of the ring currents is calculated from the tables of Johnson and Bovey (21), corrected, and used to predict values of the chemical shifts. The AA'BB' analysis is carried out on the spectrum of triptycene, and experimental chemical shifts compared with predicted values.

The effect of the ring currents at the bridgehead hydrogen is calculated from the tables of Johnson and

Bovey (21) and corrected. This quantity is used to correct the experimental value of the chemical shift for the magnetic anisotropy arising from the ring currents. This last value is then used to calculate the C^{13}-H coupling of the bridgehead hydrogen after the manner of Goldstein and Reddy (46).

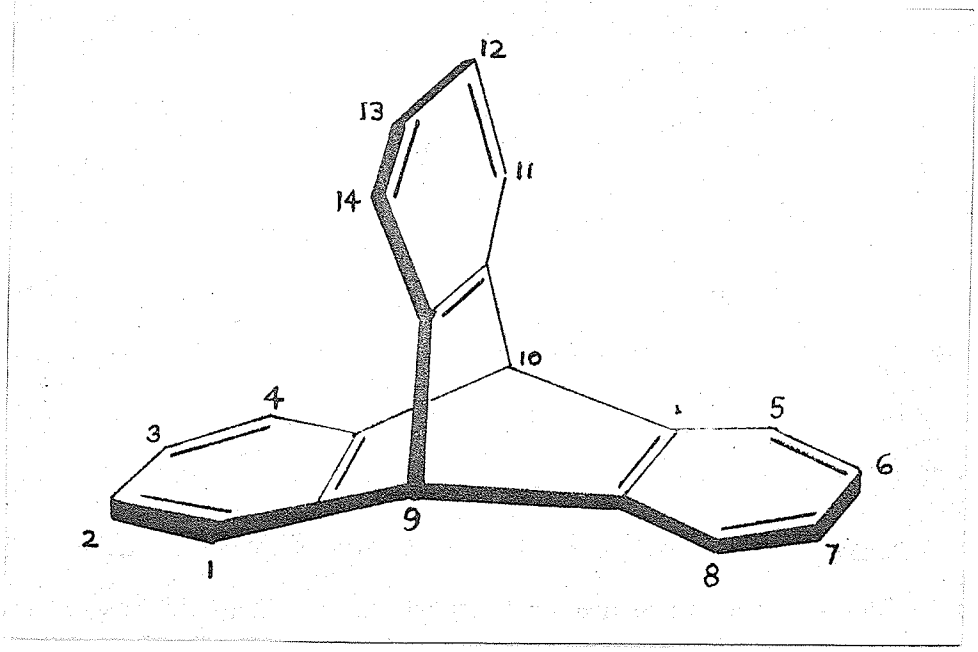

Figure 14: The triptycene molecule.

Chapter VII

EXPERIMENTAL METHODS

EXPERIMENTAL METHODS

All spectra were obtained at 25° C. using a Varian DA 60I spectrometer operating at 60 Mc/sec., and locked onto internal tetramethyl silane. Spectra were taken on the frequency sweep mode. Calibrations were placed on the spectra using a Hewlett Packard audio oscillator and measured by means of a Hewlett Packard electronic counter. Decoupling was carried out using a Hewlett Packard audio oscillator. All samples were contained in cylindrical glass sample tubes of 4 mm. inner diameter and 5 mm. outer diameter. The results are the average of four runs.

A saturated solution (2.2 mole per cent) of triptycene in carbon disulfide was used. Solutions were sealed in the sample tubes after degassing on the vacuum line. The triptycene used was a commercial product.

The spectrum of a solution (2.4 mole per cent) of benzene in carbon disulfide was taken under the same experimental conditions as that of triptycene. The results are the average of four runs.

Chapter VIII

EXPERIMENTAL RESULTS

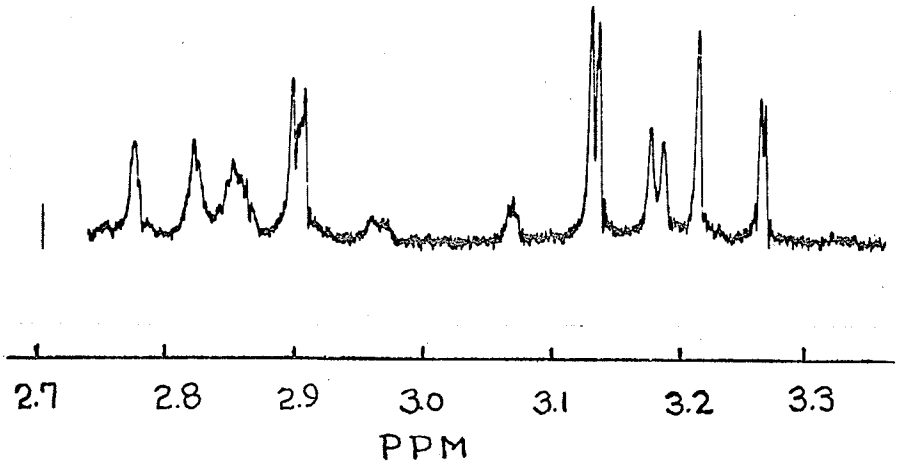

Figure 15a: Simple spectrum of triptycene.

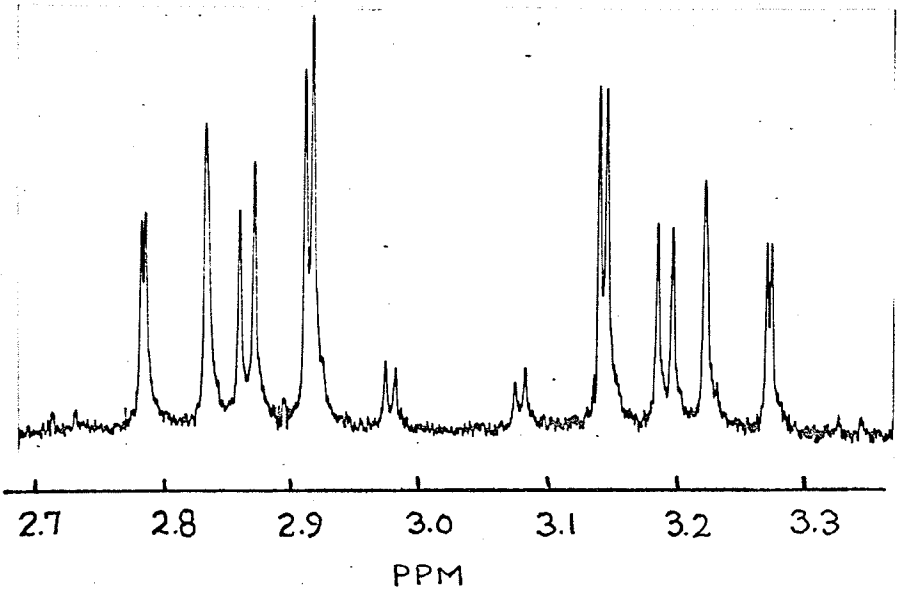

Figure 15b: Decoupled spectrum of triptycene.

Figure 16a: Line assignment of the triptycene spectrum according to Dischler and Englert (44).

b: Line assignment of the triptycene spectrum according to Lim, Taurins and Whitehead (45).

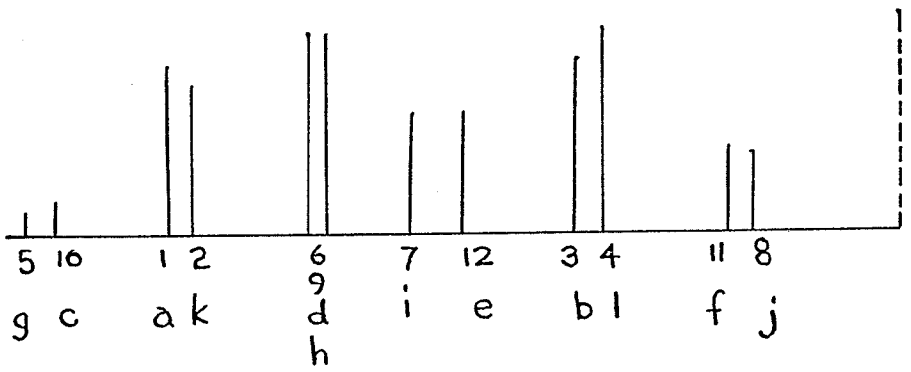
5 10 1 2 6 9 7 12 3 4 11 8
g c a k d h i e b l f j

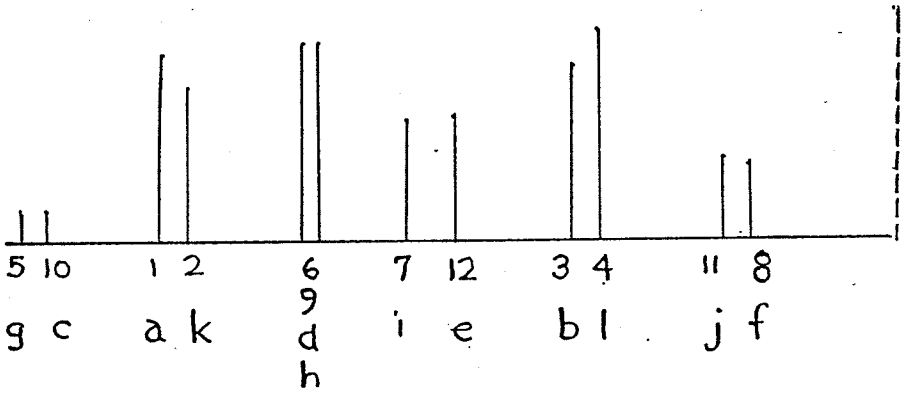
5 10 1 2 6 9 7 12 3 4 11 8
g c a k d h i e b l j f

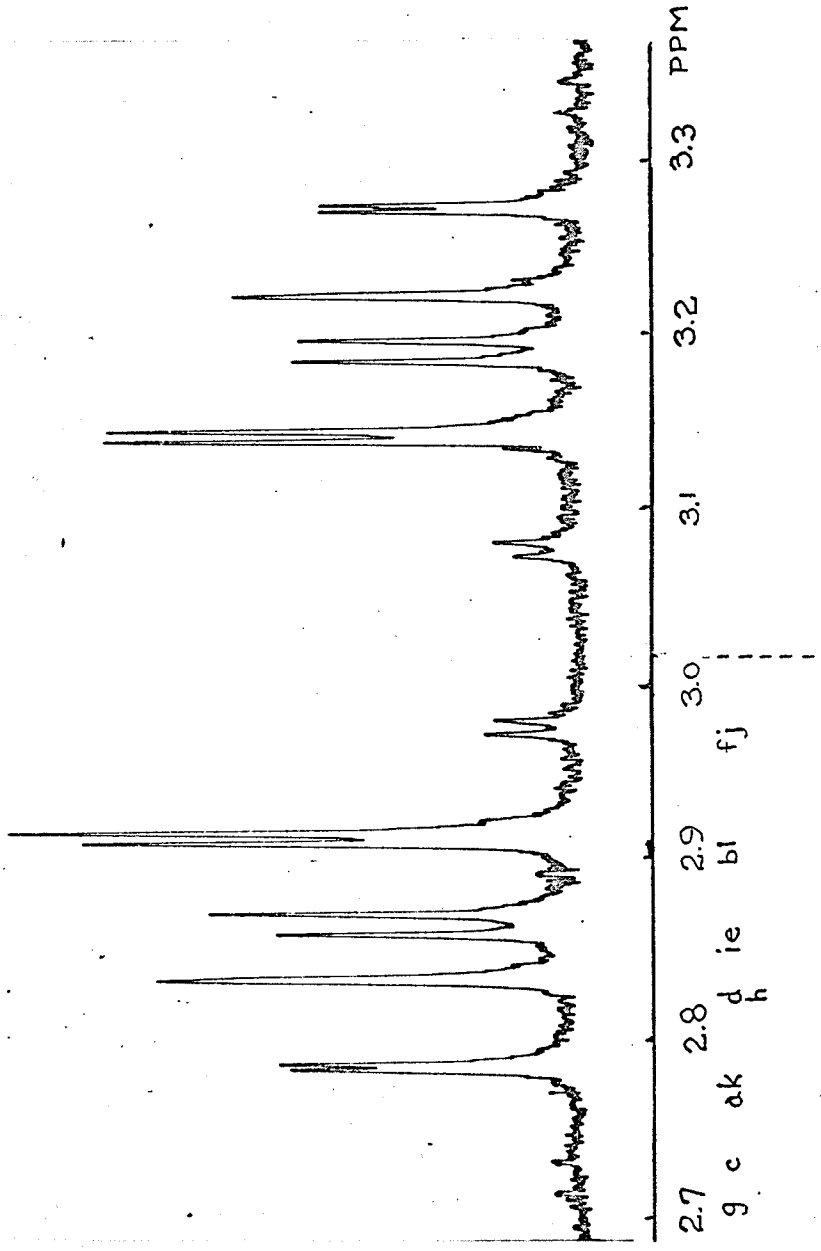

Figure 17: Line assignment of triptycene spectrum.

Figure 18: Experimental values for the chemical shifts of the A and B ring protons of triptycene (saturated solution) measured on the τ scale. The two shifts are placed symmetrically about the position of the center of the ring proton spectrum.

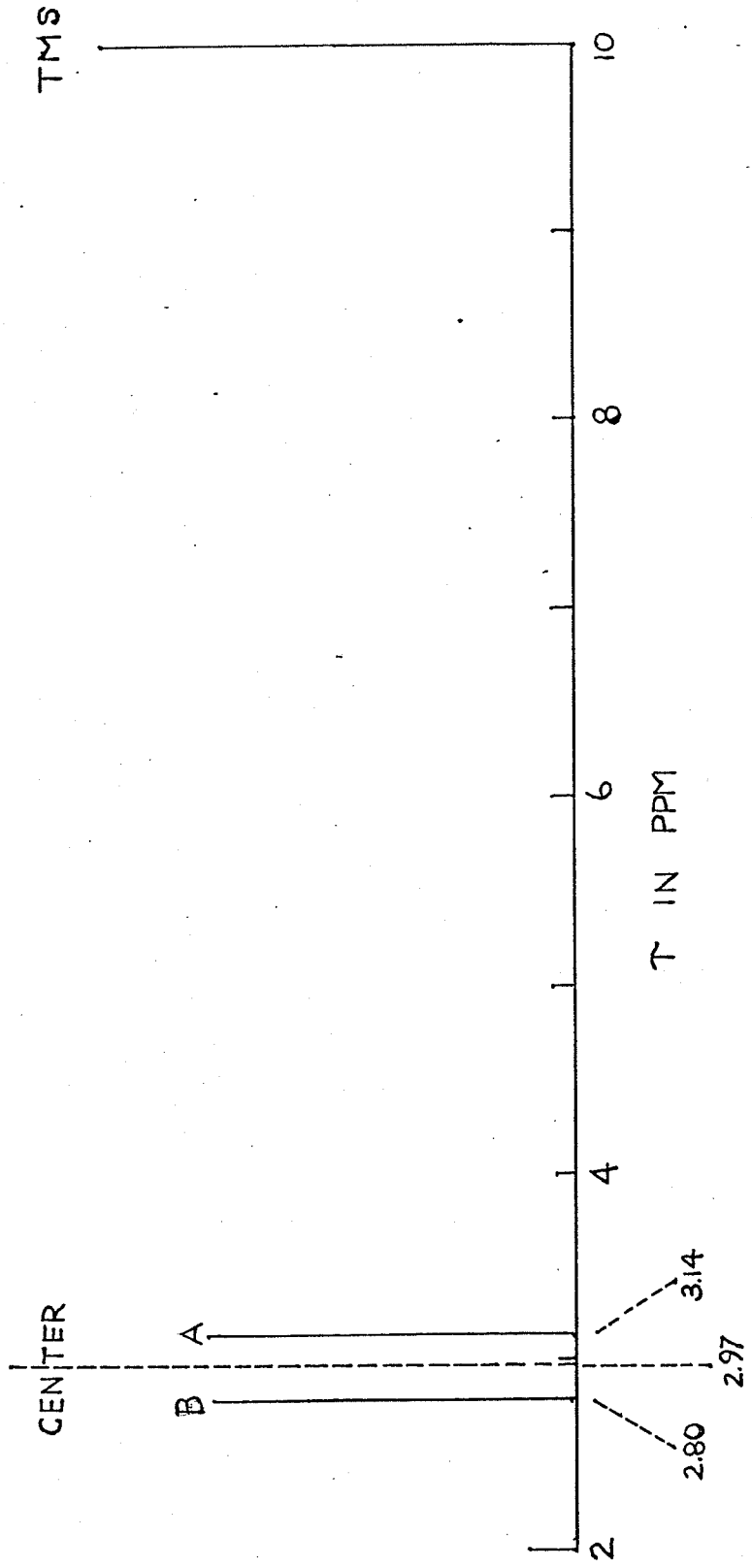
TMS
10
8
6
4
2
τ IN PPM
CENTER
A
B
3.14
2.97
2.80

Figure 19a: Line positions and intensities predicted from the relations of Table I using values for the parameters determined from experimental spectra. (The values of the graph are listed in Table VIII).

b: Line intensities measured from experimental spectra. (The values of the graph are listed in Table VIII).

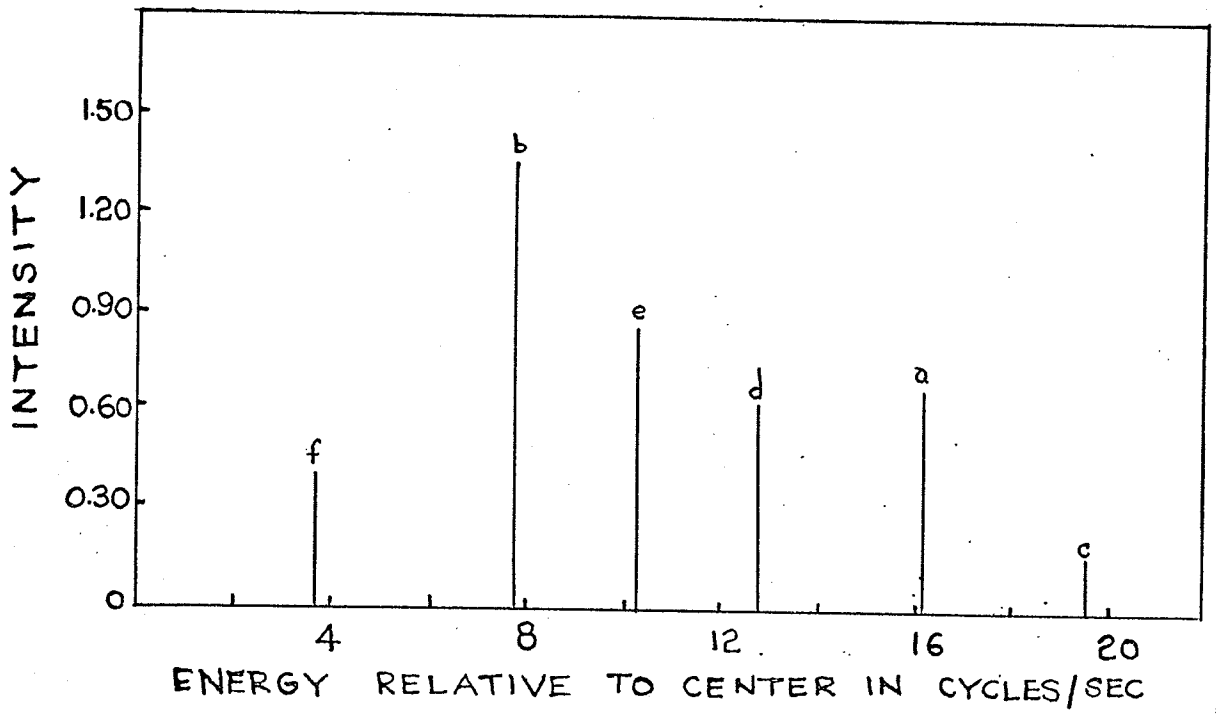
INTENSITY
1.50
1.20
0.90
0.60
0.30
0
b
e
d
a
f
c
4
8
12
16
20
ENERGY RELATIVE TO CENTER IN CYCLES/SEC

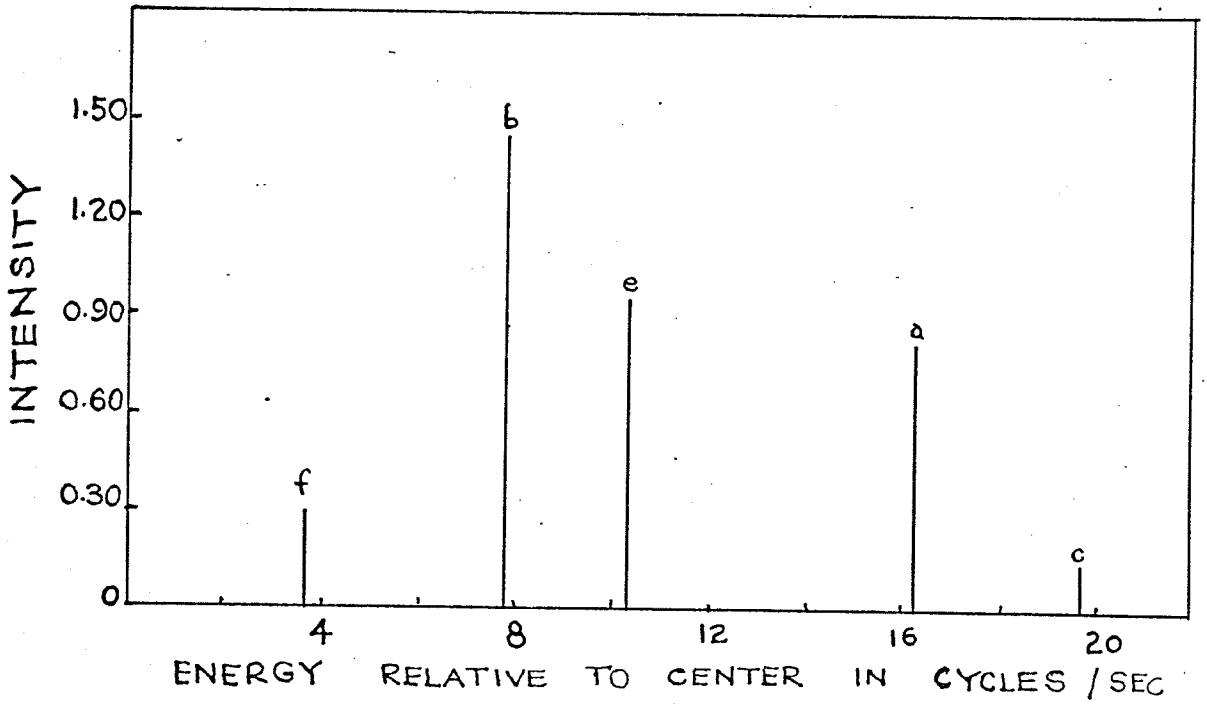
INTENSITY
1.50
1.20
0.90
0.60
0.30
0
b
e
a
f
c
4
8
12
16
20
ENERGY RELATIVE TO CENTER IN CYCLES / SEC

Table II

INTENSITIES AND ENERGIES RELATIVE THE CENTER OF THE BAND OF THE AA'BB' PORTION OF THE TRIPTYCENE SPECTRUM

Line assignment	Energies (Line positions) cycles/sec.	Intensities ($\Sigma I = 8$)
g	20.87 ± 0.14	0.06 ± 0.01
c	19.67 ± 0.09	0.08 ± 0.01
a	16.22 ± 0.08	0.79 ± 0.02
k	15.96 ± 0.07	0.83 ± 0.03
h	12.84 ± 0.09	1.11 ± 0.04*
d	12.84 ± 0.09	
i	11.13 ± 0.10	0.84 ± 0.03
e	10.35 ± 0.12	0.93 ± 0.05
b	7.79 ± 0.09	1.38 ± 0.09
l	7.40 ± 0.07	1.49 ± 0.03
f	3.62 ± 0.10	0.27 ± 0.02
j	3.11 ± 0.10	0.23 ± 0.02

* d and h are indistinguishable.

Table III

COMPARISON OF PARAMETERS EVALUATED BY DIFFERENT COMBINATIONS OF LINE ENERGIES (AN INTERNAL CHECK)

Parameter	Equation used	Value cycles/sec.
K	(68a)	8.16
	(68b)	8.15
	(68c)	8.12
	(68d)	8.19
C	(69a)	24.01
	(69b)	23.98
	(69c)	23.97
G	(72a)	9.22
	(72b)	9.22
$\nu_o \delta$	(76a)	22.48
	(76b)	22.36

Table IV

EVALUATION OF C, D, F, G AND $\nu_o \delta$

Parameter	Equation used	Value cycles/sec.
C	(89)	23.99
D	(70)	30.02
F	(71)	16.46
G	(90)	9.22
$\nu_o \delta$	(91)	22.42

Table V

EVALUATION OF N, K, L, M

Parameter	Equation used	Value cycles/sec.
N	(75a)	8.43
K	(88)	8.16
L	(73)	5.90
M	(74)	7.01

Table VI

SUMMARY OF THE CHEMICAL SHIFT AND COUPLING CONSTANTS

Parameter	Equation used	Value cycles/sec.
J_{12}	(92)	7.58
J_{13}	(93)	7.21
J_{14}	(94)	1.22
J_{34}	(95)	0.57
$\nu_o \delta$	(91)	22.42

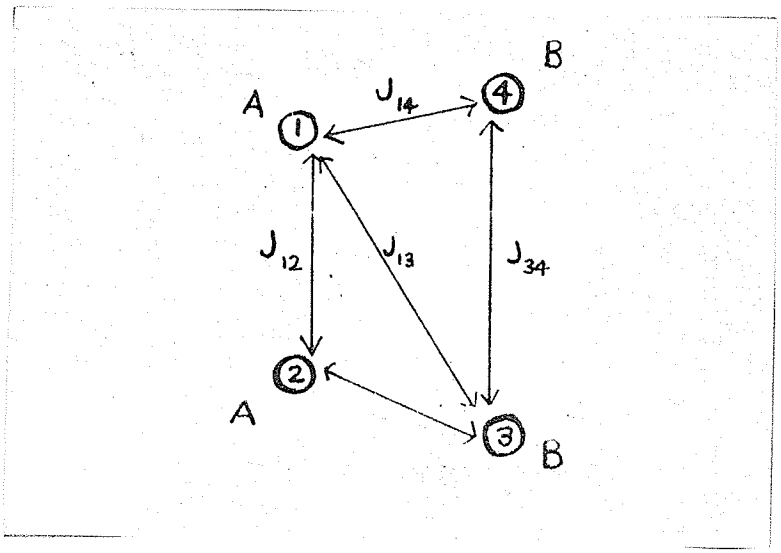

Figure 20b: Triptycene: definition of terms.

Table VII

COMPARISON OF THEORETICAL AND OBSERVED INTENSITIES

Intensity Expressions	Theoetical Value	Experimental Value
$I_a + I_b$	2	2.17
$I_c + I_e$	1	1.01
I_a/I_b	0.48	0.57

Theoetical	Experimental
$I_k \simeq I_a$	$I_k = 0.83;\ I_a = 0.79$
$2 \leq I_k + I_l \leq 3$	$I_k + I_l = 2.31$

Table VIII

PARTIAL AA'BB' SPECTRUM, CALCULATED AND EXPERIMENTAL

Line	Energies (cycles/sec.) Calculated	Experimental
a	16.21	16.22
b	7.78	7.79
c	19.62	19.67
d	12.84	12.84
e	10.40	10.35
f	3.62	3.62

	Intensities Calculated	Experimental
a	0.65	0.79
b	1.35	1.38
c	0.16	0.08
d	0.61	-
e	0.85	0.93
f	0.40	0.27

A - TRIPTYCENE RING PROTONS

The proton system of triptycene (Figure 14) is classified AA'BB'. The observable spectrum thus consists of twenty-four lines as outlined in Chapter IV. The initial spectrum of the ring proton system is displayed in Figure 15a. The low field half of the spectrum shows noticeable line broadening as does the high field half to a smaller extent. This line broadening was attributed to coupling arising from interaction of ring protons with the bridgehead protons. A decoupled spectrum was taken by irradiating the line position of the bridgehead protons. The resulting spectrum (Figure 15b) consisted of sharp, very well defined lines with line splittings as small as 0.25 cycles/sec. (.004 p.p.m.) observable in both halves of the spectrum.

Assignment of line positions to transition energies was rendered uncertain by a lack of agreement in the assignment of AA'BB' cases treated by different authors. Among the earliest AA'BB' systems treated is an analysis of the naphthalene spectrum by Pople, Schneider and Bernstein (54) who developed the assignment from the AA'XX' system. Unfortunately, the work was carried out at 40 Mc./sec. and cannot be used for direct comparison. Dischler and Englert (44) treated

a series of AA'BB' spectra and the assignment they used is shown in Figure 16a. Lim, Taurins and Whitehead (45) carried out the AA'BB' analysis with a computer program described in Chapter IV. Their assignment shown in Figure 16b gives the best agreement in all cases treated by them.

The assignment of Lim et al (Figure 16b) differs from that of Dischler and Englert (Figure 16a) only in the assignment of lines "j" and "f". The method of Lim et al was more rigourous than that of Dischler et al, and the assignment of the triptycene spectrum that was used in this analysis was that of Lim et al (Figure 17).

The value of the line positions "a" to "l" relative to the center of the spectrum are summarized in Table II. All numbers represent an average over both halves of four spectra. Errors listed are mean deviations. The line positions were used to calculate values of the parameters K, L, M, N and $\nu_o\delta$ (subsequent, in certain cases, to the determination of C, D, F and G). Inspection of equations (68a) to (76b) of Chapter IV indicates that in the cases of K, C, G and $\nu_o\delta$ there is more than one way to evaluate the parameter. The multiple values obtained for these parameters are listed in Table III and serve as an indication of the

consistency of the system.

Where necessary the value assigned to a parameter was obtained by averaging multiple equations - thus from equations (68a - d)

(88) $K = b - a + k - l + 1/2\ (g + i - h - j)$,

from equations (69)

(89) $C = 1/3\ (a + b + g + j + h + i)$,

from equations (72a - b)

(90) $G = 1/2\ (c - e + d - f)$,

and from equation (76a - b)

(91) $\nu_o\delta = 1/2\left[\sqrt{4ab} + \sqrt{2(ce + df)}\right]$.

The values of parameters C, D, F, G and $\nu_o\delta$ are listed in Table IV. Parameter C was calculated from equation (88), D was calculated from equation (70), F from equation (71), G from equation (90) and $\nu_o\delta$ from equation (91). Using the data of Tables II and IV, parameters N, K, L and M were calculated from equations (75a), (88), (73) and (74), respectively. These values are listed in Table V.

Table VI lists the values of the coupling constants of the ring protons, J_{12} , J_{13} , J_{14} , J_{34} and the chemical shift $\nu_o\delta$ between the A and B protons. The coupling constants were calculated from equations (66a - d):

(92) $J_{12} = 1/2\ (K + M)$

(93) $J_{13} = 1/2\ (N + L)$

(94) $J_{14} = 1/2\ (N - L)$

(95) $J_{34} = 1/2\ (K - M)$

The assignment of values of the coupling constants must also be accompanied by the assignment in the triptycene molecule of the class A and class B protons. Equation (66d) requires

(66d) $M = (J_{12} - J_{34}) \geq 0;\ J_{12} \geq J_{34}.$

The ring protons of triptycene are shown in Figure 20.

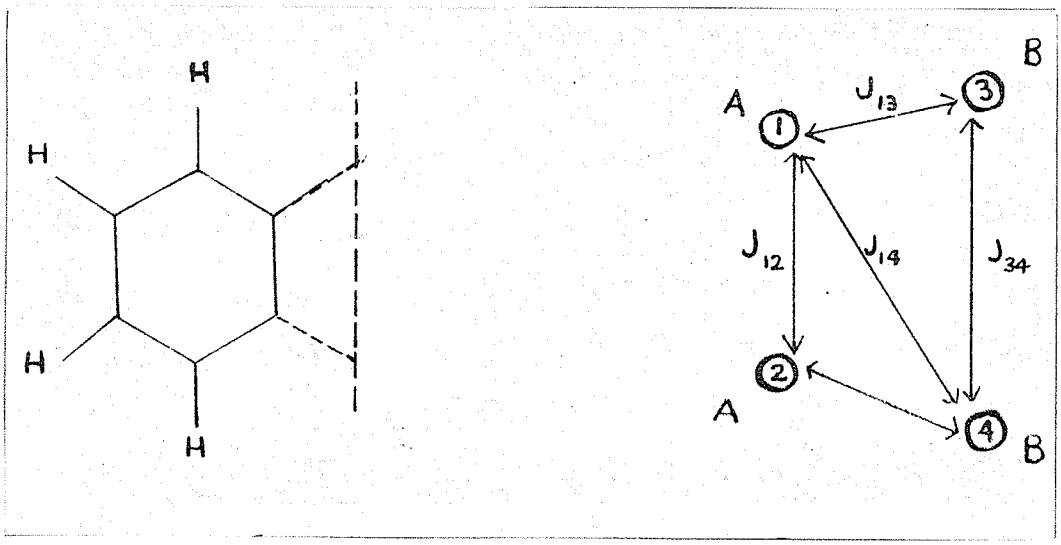

Figure 20: Assignment of triptycene ring protons.

The two para protons belong to one class, the remaining ortho protons belong to the other. Comparison with

Figure 13 indicates that one of $J_{12} = J_{AA}$ or $J_{34} = J_{BB}$ is a para coupling while the other is an ortho coupling. Ortho coupling is known to be greater than para coupling; therefore, since $J_{12}(J_{AA}) \geq J_{34}(J_{BB})$, the A protons must lie ortho to one another, while the B protons lie para. This assignment is shown in Figure 20.

Figure 18 shows the assignment, on the τ scale, of the chemical shift of A protons and B protons relative to tetramethyl silane. The A and B halves of the spectrum lie symmetrically on either side of the center of the band, separated by a chemical shift of $\nu_o \delta$. The B protons by reason of molecular geometry (Figure 20) are more strongly coupled to the bridgehead hydrogens than A protons and are therefore assigned to the low field half of the spectrum. The chemical shifts relative to tetramethyl silane were determined by calculating the position of the center of the twenty-four lines and adding $\frac{1}{2}\nu_o \delta$ to give the B chemical shift and subtracting $\frac{1}{2}\nu_o \delta$ to give the A chemical shift. The position of the center line relative to tetramethyl silane was calculated to be 422.48 ± 0.03 cycles/sec. where the error is the mean deviation. The resulting values of the chemical shifts were: B protons, $\tau = 2.77$ p.p.m. (433.7 cycles/sec.), A protons, $\tau = 3.14$ p.p.m. (411.3 cycles/sec.).

Table II contains, in addition to line energies, the experimentally determined line intensities. Table VII contains a comparison of the intensity relations of equation (77) to (82) from Chapter IV with those determined from Table II. Agreement is reasonably good when the rough nature of intensity measurements is taken into consideration.

To conclude the AA'BB' analysis, the energy levels of the AA'BB' half-spectrum were calculated with the exception of those involving the solution of the 4 x 4 determinant. Where possible, transition energies and intensities were determined using the values of N, K, L and M listed in Table V. Only six lines could be determined without a knowledge of the energy levels Ω_1, Ω_2, Ω_3, and Ω_4 (that is, without a solution to the 4 x 4 determinant). These are listed in Table VIII. Also listed in Table VIII, for comparison, are the values for the corresponding lines from the experimental spectrum. The information summarized in Table VIII is reconstructed into the two spectra shown in Figure 19.

B - BRIDGEHEAD PROTONS

The spectrum of the bridgehead hydrogens consisted of a single peak with an unresolvable shoulder. A measurement of the chemical shift gave a value of τ = 4.79 p.p.m. for the bridgehead hydrogens.

C - BENZENE

The chemical shift of benzene relative to tetramethyl silane was measured to be τ = 2.78 p.p.m.

Chapter IX

DISCUSSION OF RESULTS

Figure 21a: Experimental values for the chemical shifts of the A and B ring protons measured on the τ scale.

b: Values for the chemical shifts of the A and B ring protons predicted from the tables of Johnson and Bovey (21).

c: The values of Figure 21b corrected in accordance with the relation $\Delta\tau' = 0.63\ \Delta\tau$.

d: The values of Figure 21b corrected for substituent effects, using the ortho-xylene approximation.

e: The values of Figure 21c corrected for the substituent effect.

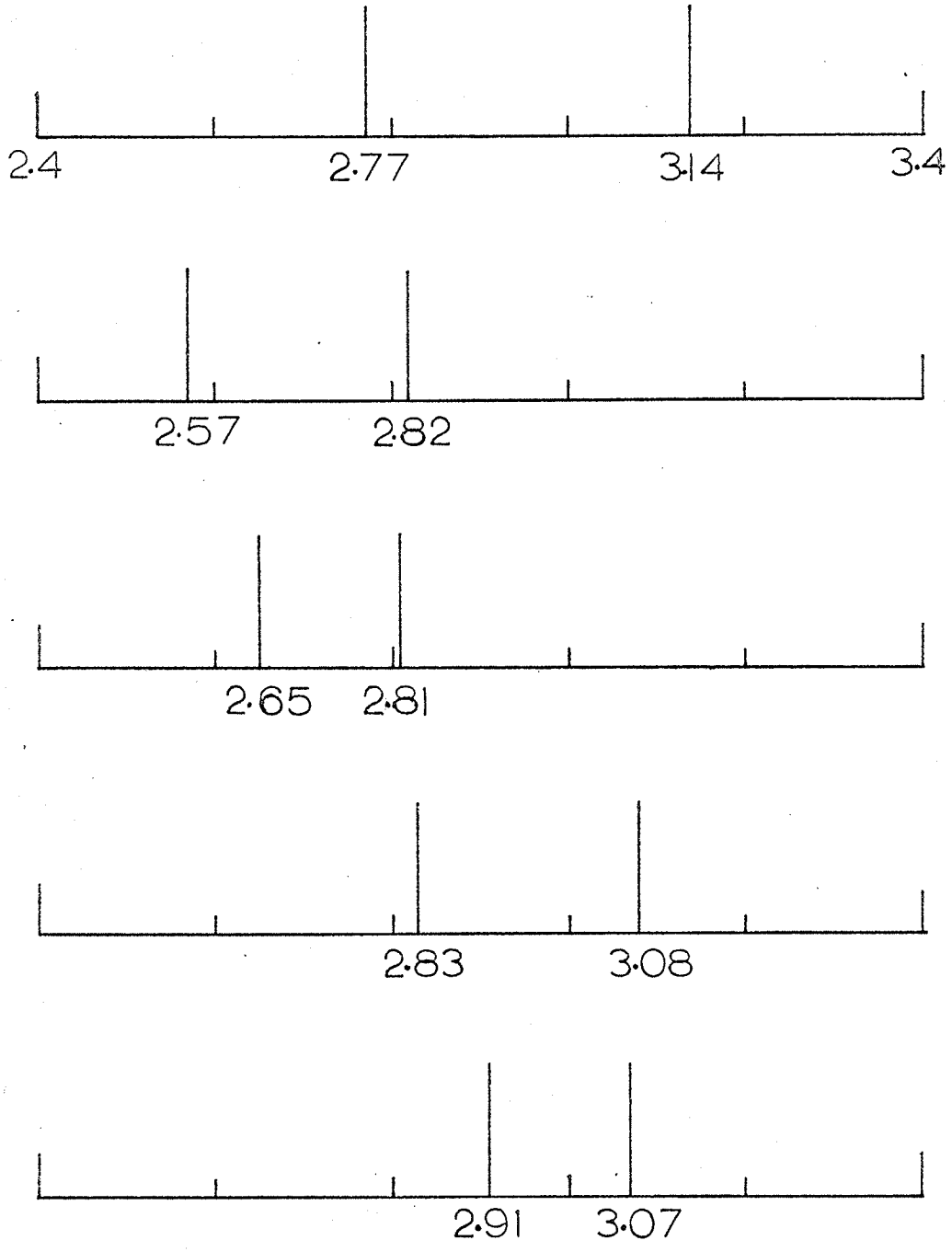
2·4
2·77
3·14
3·4
2·57
2·82
2·65
2·81
2·83
3·08
2·91
3·07
τ ppm

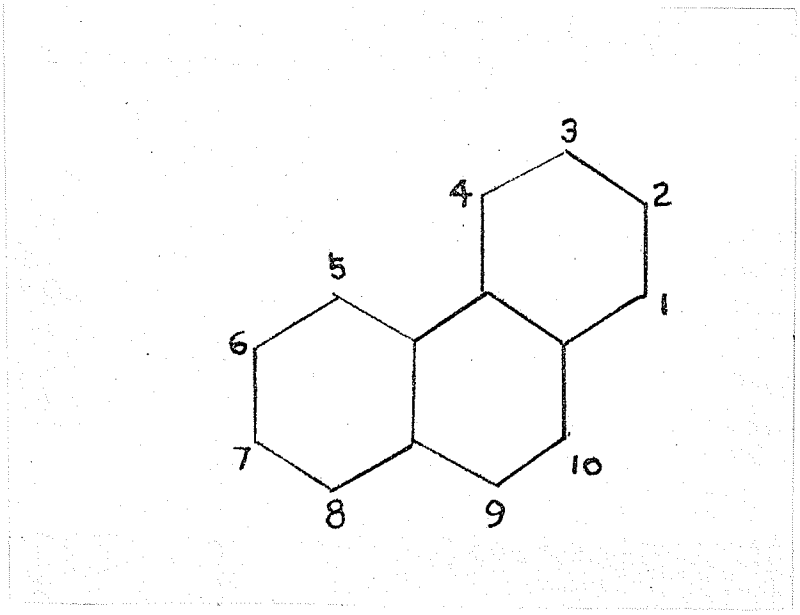

Phenanthrene

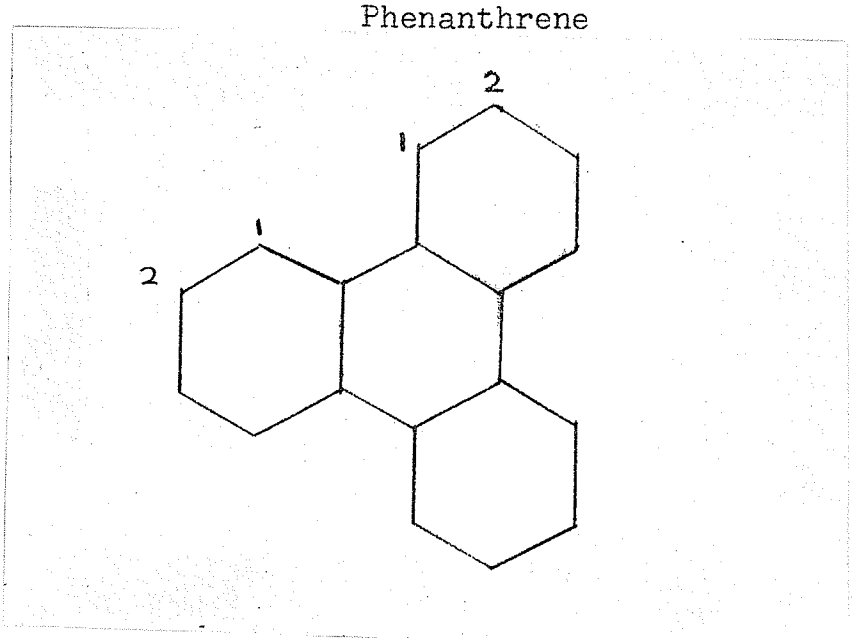

Triphenylene

Figure 22: Steric hindrance of ring protons.

Figure 23: The proton chemical shift (on the τ scale) plotted as a function of C^{13}-H coupling to the proton. The points represented by open circles taken from the data of Drago and Matwiyoff (59). The points represented by open triangles are taken from the data of Goldstein and Reddy (46). The dotted horizontal line represents the chemical shift of the bridgehead triptycene proton after a correction to remove the effects of ring current anisotropy.

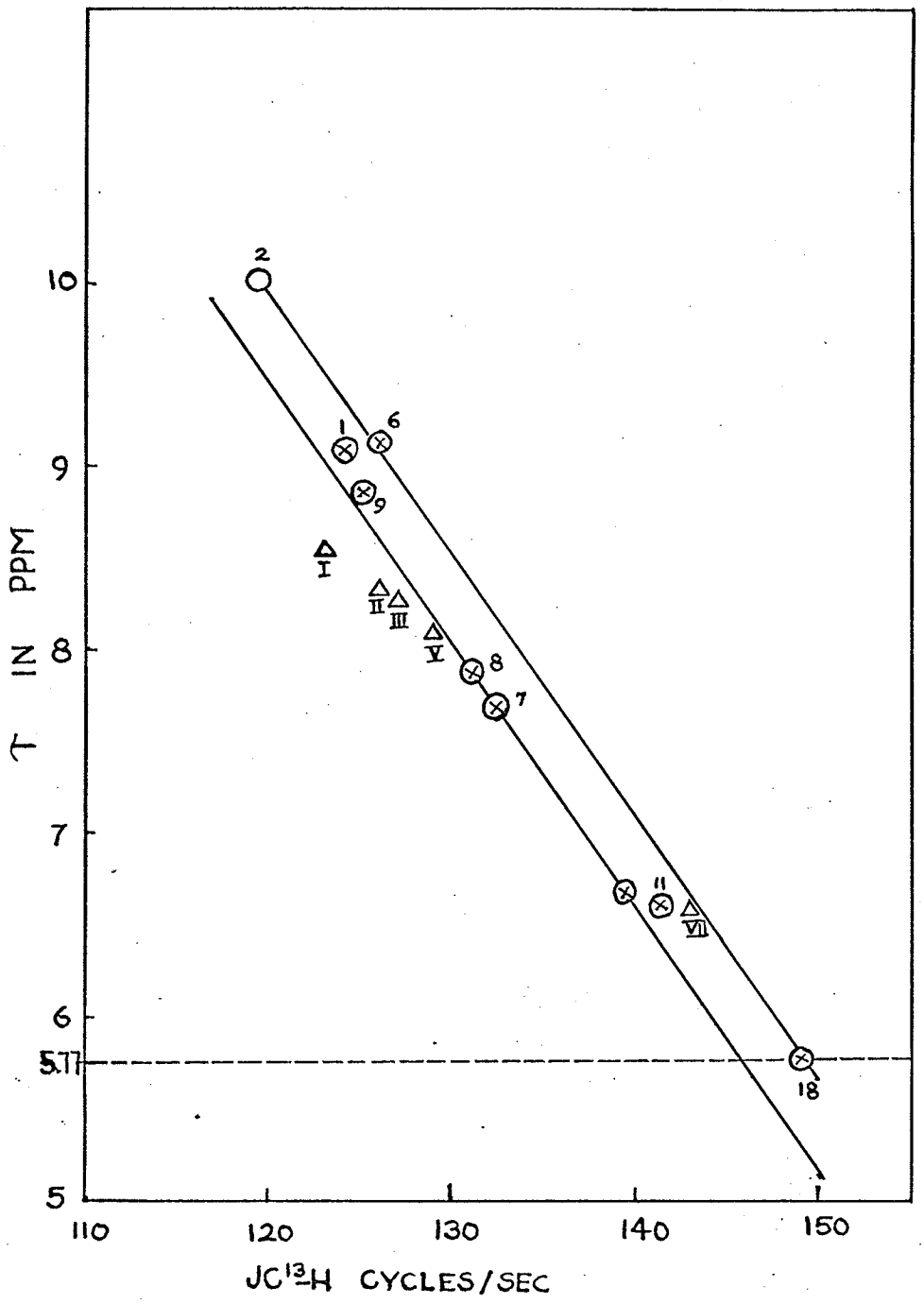
τ IN PPM
10
9
8
7
6
5.11
5
110
120
130
140
150
JC13H CYCLES/SEC
2
1
6
9
I
II
III
V
8
7
11
VII
18

Table IX

A COMPARISON OF THE ANALYSIS OBTAINED IN THIS WORK WITH THE RESULTS OF SMITH AND SHOULDERS (55)

Physical quantity	This work	Smith and Shoulders
J_{12}	7.58 cycles/sec. *	7.70 cycles/sec. †
J_{13}	7.21	7.60
J_{14}	1.22	1.20
J_{34}	0.57	0.00
$\nu_o\delta$	22.42	28.26
τ_A	3.14 p.p.m.	—
τ_B	2.80	2.72 p.p.m.
$\tau_{Bridgehead}$	4.79	4.40

* in carbon disulfide solution

† in acetone solution

Table X

ELECTRON DENSITIES OF THE $\widetilde{\pi}$ ELECTRON SYSTEM OF TRIPTYCENE (FROM APPENDIX A)

Positions (Figure 14)	Electron Density
1, 14, 8, 4, 11, 5	0.998854
2, 13, 7, 3, 12, 6	1.000094
Remaining inner carbon atoms	1.001052

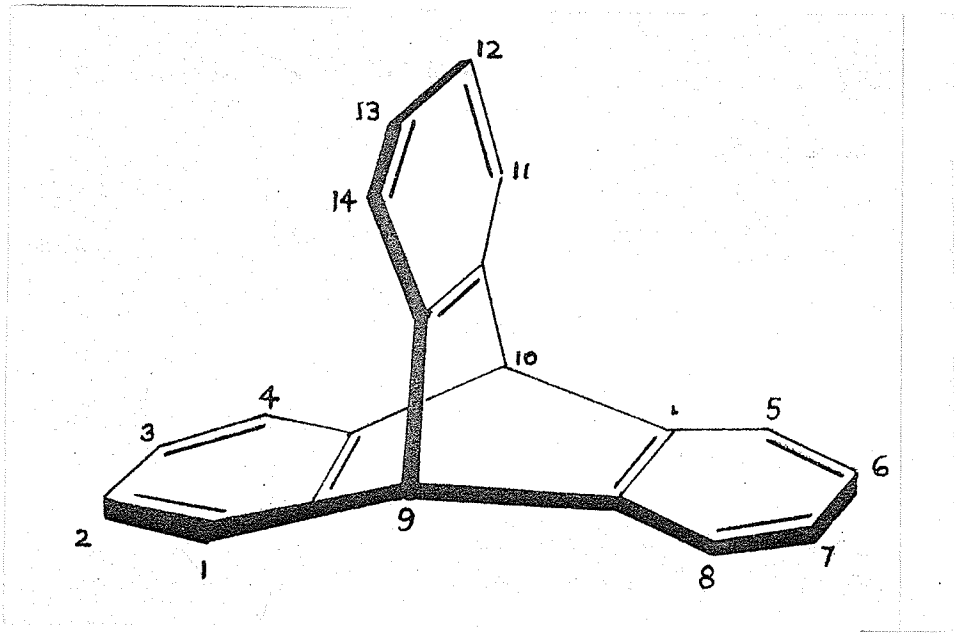

Figure 14: Triptycene molecule.

Table XI

PREDICTION OF THE CHEMICAL SHIFTS OF THE RING PROTONS OF TRIPTYCENE

a) FROM THE TABLES OF JOHNSON AND BOVEY

Class of proton	$\Delta\tau$ (p.p.m.)	τ (p.p.m.)
A	+0.04	2.82
B	-0.21	2.57

b) CORRECTED BY THE MULTIPLICATIVE FACTOR 0.63

Class of proton	$\Delta\tau'$ (p.p.m.)	τ' (p.p.m.)
A	+0.03	2.81
B	-0.13	2.65

c) τ CORRECTED BY SUBSTITUENT EFFECT

Class of proton	Substituent effect (p.p.m. on τ scale)	τ'' (p.p.m.)
A	+0.26	3.08
B	+0.26	2.83

d) τ' CORRECTED BY SUBSTITUENT EFFECT

Class of proton	Substituent effect (p.p.m. on τ scale)	τ''' (p.p.m.)
A	+0.26	3.07
B	+0.26	2.91

A - INTRODUCTION

The nuclear magnetic resonance spectrum of triptycene has been analyzed previously by Smith and Shoulders (55). The previous analysis was made on spectra lacking the resolution and line separation of the present spectra. In addition, the analysis by Smith and Shoulders assigns a value of zero to the para coupling. A value for the para coupling of 0.57 cycles/sec., obtained in the present work, is more reasonable in view of the range of known para couplings of protons on the aromatic ring. Smith and Shoulders' results are compared with the present work in Table IX. It is important to note that Smith and Shoulders' results were given for an acetone solution while the present work gives results for a carbon disulfide solution.

The large ring system of the triptycene molecule suggests the application of ring current theory in an attemptto evaluate anisotropy effects.

Smith and Shoulders have reported a value of 145 cycles/sec. for C^{13}-H coupling constant of the bridge-head proton which they considered too high. The method of Goldstein and Reddy (46) is used to predict a value for the coupling constant which supports their experimental value.

B - THE CHEMICAL SHIFT OF THE RING PROTONS

The triptycene molecule (Figure 14) contains three aromatic rings. Each can produce a ring current as outlined in Chapter II, Section C, Part 1. The tables of Johnson and Bovey (21) for the calculation of anisotropy effects assume a ring current equal to that in the benzene molecule. As was pointed out by Pople (23) the ring currents in the various rings of a polycyclic compound are not all equal to that of benzene. It is possible (23) to calculate the ring current relative to benzene by a molecular orbital method. Therefore, before applying the tables of Johnson and Bovey, a molecular orbital calculation was made to determine whether there was any overlap between the aromatic rings.

A Hückel type molecular orbital calculation was made on the π electron system using a linear combination of symmetry orbitals as outlined by Cotton (53) for bicyclooctatriene. The overlap of the π electron system between rings can occur only at those sites of the triptycene molecule which correspond to bicyclooctatriene. The detail of the calculation is given in Appendix A. The results, summarized in Table X, indicate that the largest change effected in the π electron density is a decrease

from 1.0000 to 0.9989 (a change of 0.0011). It was assumed that any change of ring current would be negligible. The ring current in the triptycene rings was assumed to be equal to that of benzene.

The chemical shift was estimated for both classes of ring proton in the triptycene molecule. The ring current effect due to the two opposite rings occurs in addition to the effect of the ring on which the protons are situated. Johnson and Bovey's tables were used to calculate this shift, $\Delta\tau$, by the two opposite rings. Appendix B describes the calculations; Table XIa lists the predicted values of the chemical shifts of the ring protons τ_A and τ_B. The chemical shifts were obtained by adding $\Delta\tau_A$ and $\Delta\tau_B$ to the experimental τ value of benzene, 2.78 p.p.m. Figure 21b compares the predicted chemical shifts of Table XIa with experimental values (Figure 21a).

In the description of ring current theory in Chapter II, it was pointed out that Jonathon, Gordon and Dailey (25) had observed a systematic discrepancy between experimental and calculated (that is, predicted) chemical shifts. This discrepancy can be formulated by the relationship noted by Dailey (56)

$$(60) \qquad \Delta\sigma_{exp'l} = 0.63\,\Delta\sigma_{calc'd} - 0.13 \ .$$

As seen from the graph of Figure 10, there is considerable scatter of data about the straight line, and the equation (60) can be used only to give a rough correction for the inadequacies of ring current theory. It should, however, be noted that the two points (1.44, 1.38) and (1.29, 1.34) which lie considerably off the straight line pertain to the 4 and 5 positions of phenanthrene and the 1 position of triphenylene (Figure 22), respectively. Inspection shows that there is steric hindrance of the protons involved. Strong Van der Waals interaction can occur between these protons resulting in a decrease in the shift δ (an increase in τ). In the case of phenanthrene, this shift was shown to be of the order of 0.5 p.p.m. (57). None of the protons of triptycene are sterically hindered, and a large discrepancy from equation (60) due to Van der Waals shift is unlikely.

Equation (60) cannot, however, be used in its entirety. The best relationship fitting the data of Figure 10 is a straight line which intercepts the y axis at (0, -0.13). This does not hold for $\Delta\sigma$ small and approaching zero. $\Delta\sigma$ is the chemical shift relative to benzene, and for benzene both $\Delta\sigma_{\text{calc'd}}$ and $\Delta\sigma_{\text{exp'l}}$ are zero. Clearly, any line which fits data for small $\Delta\sigma$ must pass through the origin. The ring current theory gave $\Delta\tau_A = +0.04$ and $\Delta\tau_B = -0.21$ for the ring protons

(where $\Delta\tau = -\Delta\sigma$). Both these values are much smaller than the chemical shifts given in the data of Jonathon, Gordon and Dailey. The constant term -0.13 is comparable to the value of $\Delta\tau$ and is not applicable to values so close to the origin. The multiplicative term may or may not apply for such values.

To illustrate the case in which the multiplicative portion of equation (60) holds for the triptycene ring protons, Table XIb lists the values of τ_A' and τ_B' obtained by adding $\Delta\tau'$ to the chemical shift of benzene where $\Delta\tau'$ is calculated from the relation

$$\Delta\tau' = 0.63\ \Delta\tau$$

The chemical shifts τ_A' and τ_B' are compared with experimental values in Figure 21c.

In addition to the effects of ring currents, a substituent effect must be accounted for. In the case of triptycene, the substituents are the two C-H groups held fixed in orientation. In both cases, the carbon is attached to three benzene rings and, ideally, the substituent effect should be estimated from a molecule such as triphenyl methane. Unfortunately the ring currents present in such molecules make it impossible to isolate a substituent effect. For lack of a better approximation, the chemical shift observed between benzene and ortho-xylene was taken to approximate the substituent effect of triptycene.

From the table compiled by G. V. D. Tiers (58) τ(benzene) = 2.73 p.p.m., τ(ortho-xylene) = 2.99 p.p.m. and the chemical shift is +0.26 p.p.m. on the τ scale. This value was added to τ_A and τ_B. The resulting shifts τ_A'' and τ_B'' are listed in Table XIc and illustrated in Figure 21d. The substituent effect was also added to τ_A' and τ_B' to give τ_A''' and τ_B''' as listed in Table XId and illustrated in Figure 21e. The results shown in Figure 21a - e indicate that good agreement is not possible with any of the cases considered. The number of the factors contributing to the chemical shift is such that any attempt to localize the failure is inconclusive. The discrepancy between predicted and experimental values is due either to a failure of the ring current model, inaccuracy of the substituent approximation, or some other effect not considered in this work. Smith and Shoulders' (55) suggestion of an "around the barrel" current perpendicular to the face of the rings falls in the last category. In view of the molecular orbital calculation of Appendix A, however, such an effect seems unlikely. Figure 21a - e shows that the predicted separation of the line positions of the two classes of protons is too small in all cases. Since ortho-xylene gives a spectrum of a single line (see reference 59), it can be assumed that the substituent effect does not contribute to the separation, but rather

alters the shift of ortho, meta and para protons by the same amount. The ring current model is then the alternative source of error. Figure 21d (Table XIc) indicates that the ring current effect predicted by the tables of Johnson and Bovey gives better agreement than the values given after the correction $\Delta\tau' = 0.63\Delta\tau$. This indicates that for low values of the ring current effect, the corrective equation (equation 60) is inapplicable in its entirety. Perhaps another simple correlation exists which could be used to give a better estimate for ring current effects for small effects, but data is required for a larger number of cases before a generalization can be made.

C - C^{13}-H COUPLING CONSTANT OF THE BRIDGEHEAD GROUP

The experimental value for the chemical shift of the bridgehead proton was determined to be $\tau = 4.79$ p.p.m. A calculation of the ring current shielding from the Johnson and Bovey tables gives a value for $\Delta\tau$ of -0.65 p.p.m. for each ring. The total effect for the three rings is $\Delta\tau = -1.95$ p.p.m. This value for $\Delta\tau$ places $\Delta\sigma$ (equal +1.95 p.p.m.) in the range of data given in Figure 10. It is assumed that the linear relationship is applicable and $\Delta\tau$ is corrected on the basis of equation (60). The resulting value $\Delta\tau' = -0.98$ p.p.m. should represent fairly accurately the change in chemical shift (on the τ scale) due to ring currents. An estimation of the value of the chemical shift of the bridgehead proton in the absence of ring current is obtained by subtracting $\Delta\tau'$ from $\tau = 4.79$ p.p.m. to give a value of 5.77 p.p.m.

Chapter V of this thesis gave an outline of the empirical relation between C^{13}-H coupling constants and proton chemical shifts described by Goldstein and Reddy (46). An application of this relationship to the problem of determining the C^{13}-H coupling constant would require a graph of C^{13}-H coupling constants plotted against the chemical shift for a series of similar compounds. Ideally the graph would consist of data from a series of molecules which: a) have the same hybridization, b) have the C^{13}

atom of the C^{13}-H bond attached to three other carbon atoms, c) have no heavy nucleus substituents (for reasons outlined in Chapter V) and d) do not contain ring structures which introduce anisotropy considerations. The required data is not available, but Drago and Matwiyoff (60) have measured the C^{13}-H couplings for various CH_3X compounds. The graph of Figure 23 was obtained by choosing from the data of Drago and Matwiyoff values for molecules in which X is not a heavy substituent. In addition, data from the tables of Goldstein and Reddy are also shown for the case of sp^3 molecules in which there is no aromatic ring. The molecules chosen from Goldstein and Reddy's table were: cyclohexane, isobutylene, α-methyl vinyl methyl ether (α), crotonaldehyde and α-methyl vinyl methyl ether (methoxy). Although the latter series contains secondary carbon atoms (Drago and Matwiyoff dealt only with primary carbon structures), the lines from the two graphs are very similar. Although not identical they lie close enough together to support the concept that the line is a general one for sp^3 hybridized carbon. In the absence of anisotropy the graph should give an estimate of the C^{13}-H coupling constant for given τ.

The chemical shift of the bridgehead positions altered by the removal of anisotropy effects is τ = 5.77 p.p.m. This value is shown in Figure 23 as a dotted line at τ = 5.77 p.p.m. The intersection of the dotted

line with the graph indicates that a value of 145 cycles/sec. or higher is reasonable for the C^{13}-H coupling constant.

Chapter X

SUMMARY AND CONCLUSIONS

SUMMARY AND CONCLUSIONS

The nature of the results obtained in this work are such that actual conclusions about the ring current theory itself are not warranted. The ring current theory predicted trends and relative values correctly, but was unable to predict absolute values with sufficient certainty to indicate a general value in predicting chemical shifts from first principles. It was, however, possible to obtain some agreement for the shifts of A, B and bridgehead protons within a framework of reasonable assumptions.

The literature available on application of ring current theory (56) indicates that best agreement should be found by altering the values of $\Delta\tau$, predicted by the Johnson and Bovey tables (21), using the correlation (equation 60) obtained from a comparison of predicted and experimental results in a variety of applications of the ring current tables. The results obtained on this basis, shown in Figure 21e, do not give very good agreement in the case of triptycene. The best agreement was obtained using the tables of Johnson and Bovey without correction by equation (60), as shown in Figure 21d.

The ring current theory, applied to triptycene, predicted the correct relative magnitudes of the chemical

shifts. The chemical shift of the A nucleus was predicted to have a greater τ value than the B nucleus. This result was verified by the fact that B protons by reason of geometry couple with the bridgehead protons, and the low field half of the spectrum was coupled. The ring current theory proved to be adequate for predictions of a non-absolute nature.

The lack of absolute agreement of predicted with experimental shifts is attributable to errors in the estimation of either the ring current effect or the substituent effect. Any explanation based on currents involving more than one ring is unlikely due to small p-orbital overlap between rings. The substituent effect is expected to alter the chemical shift of both A and B protons by the same amount. Discrepancy in predicted line separation is attributed to failure of the ring current approximation. The corrective equation applicable to the majority of data obtained from the ring current theory for polycyclic compounds is not applicable to triptycene. It's generality is, therefore, questionable.

The bridgehead proton shift after removal of the anisotropy effect predicted by ring current theory was found to fit a generalized plot of C^{13}-H coupling constant versus chemical shift for a series of sp^3 carbon compounds. The fit, however, indicates only approximate agreement for the predicted chemical shift.

APPENDIX

A - MOLECULAR ORBITAL CALCULATION OF THE π ELECTRON SYSTEM OF TRIPTYCENE

A molecular orbital calculation was carried out on triptycene to determine the effect on the electron system of orbital overlap between the rings. Without interaction between rings the triptycene electron energy diagram would be the combination of the energy levels of three benzene molecules; interaction produces only a slight modification.

Orbital overlap between rings is possible only for the six ring carbon atoms nearest the center of the molecule. The geometry and symmetry of these carbon atoms corresponds to the π electron system of bicyclo-octatriene. The calculation of molecular orbitals and energy levels of this molecule (53) was used as a guide.

The nuclei of the triptycene molecule are labelled according to the system employed for the associated hydrogens (Figure 14). The inner carbon atoms of the benzene rings are additionally labelled 15 to 20 (Figure 24). The problem is simplified by classifying as equivalent the nuclei lying at the same radius from the center axis of the molecule. Thus carbons 15 to 20 belong to Class I, carbons 1,14, 8, 4, 11, 5 belong to Class II and carbons 2, 13, 7, 3, 12, 6 belong

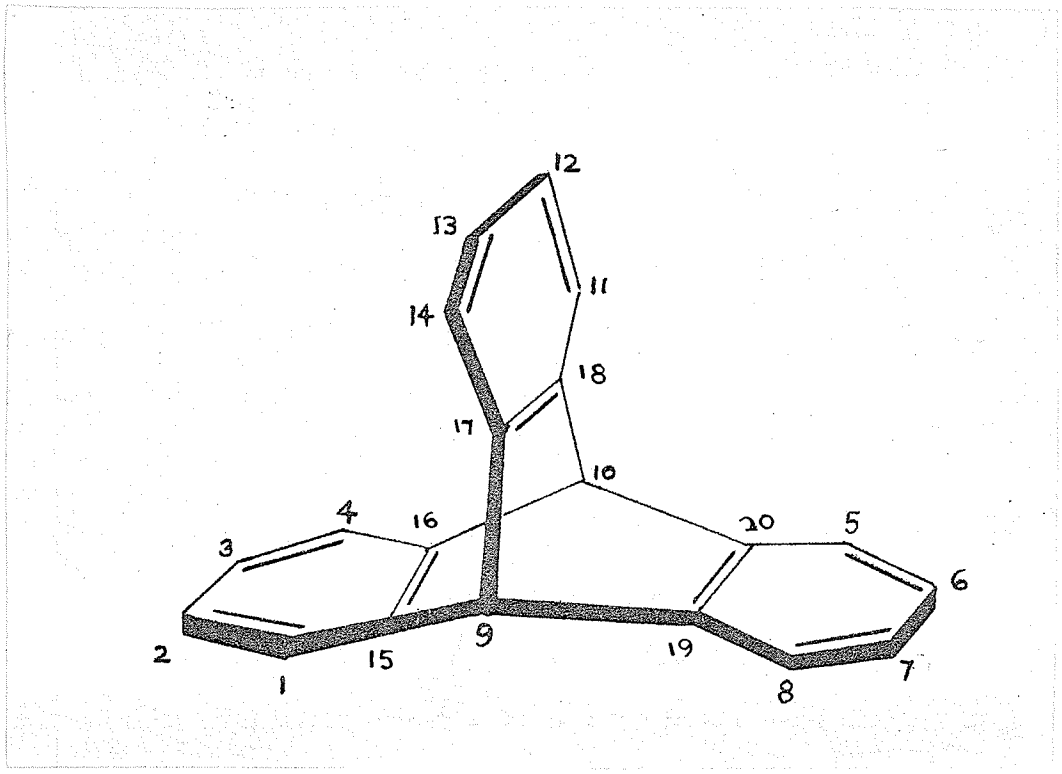

Figure 24: Numbering system of carbon atomic orbitals.

to Class III.

The molecule belongs to the symmetry group D_{3h} (as does bicyclooctatriene). The reducible representation $\Gamma_{red.}$ of the eighteen atomic p orbitals can be reduced to

(96) $$\Gamma_{red.} = 3\Gamma_{A_2'} + 3\Gamma_{A_1''} + 3\Gamma_{E'} + 3\Gamma_{E''}$$

Alternatively, the reducible representation $\Gamma'_{red.}$ of the six atomic p orbitals of each class is given by

(97) $$\Gamma'_{red.} = \Gamma_{A_2'} + \Gamma_{A_2''} + \Gamma_{E'} + \Gamma_{E''}$$

The irreducible representations of equation (96) can be used to generate a set of eighteen symmetry orbitals from the atomic orbitals. The use of symmetry orbitals results in a factored form of the 18 x 18 secular determinant derived in the Hückel method.

Alternative to setting up eighteen 18 dimensional symmetry orbitals, another set of symmetry orbitals is defined utilizing the fact that none of the symmetry operations of the D_{3h} group interchange carbon positions between classes. The alternate set consists of eighteen 6 dimensional symmetry orbitals generated by the application of equation (97) to all three classes of carbons. The symmetry orbitals used as a basis set are listed in Table XII.

The molecular orbitals are constructed as linear combinations of the 6 dimensional symmetry orbitals

$$\Psi_i = C_{i1}\psi^1_{A_2'} + C_{i2}\psi^2_{A_2'} + \cdots C_{i18}\psi^{18}_{E_b''}.$$

The determination of the coefficients C_{ij} is carried out by the variational procedure of the Huckel method. The secular equations are obtained:

$$C_{11}(H_{11} - E) + C_{12}H_{12} + \cdots C_{1\ 18}H_{1\ 18} = 0$$

$$\vdots$$

$$C_{18\ 1}(H_{18\ 1} - E) + C_{18\ 2}H_{18\ 2} + \cdots C_{18\ 18}(H_{18\ 18} - E) = 0.$$

The secular determinant is

$$(98) \quad \left| H_{ij} - \delta_{ij} E \right| = 0$$

where $H_{ij} = \psi_i \mathcal{H} \psi_j$ and E is a root of the secular equations. $\mathcal{H}$ is the Hamiltonian operator and ψ_i and ψ_j are the 6 dimensional symmetry orbitals. H_{ij} is zero unless the symmetry orbitals ψ_i and ψ_j belong to the same irreducible representation. Thus the only off diagonal elements for the matrix occur between the three symmetry orbitals of Table XII belonging to each symmetry group. The 18 x 18 determinant is factored into 3 x 3 determinants, and in determining energy levels only the 3 x 3 determinants for each symmetry group were set up.

The 3 x 3 determinants were set up using the assumptions:

$H_{ii} = \alpha$

$H_{ij} = \beta$ if i and j are adjacent on the same benzene ring

$H_{ij} = \beta'$ if i and j are adjacent on different benzene rings (Figure 25)

$H_{ij} = 0$ except for the above two cases.

Cotton (53) estimates the value of β' as 0.1β. This value was used in the present calculations. The energies were obtained by solving the 3 x 3 determinants by the Newton-Raphson method of successive approximations(61).

Table XII

p - $\widetilde{\pi}$ SYMMETRY ORBITALS

$$\psi^{1}_{A_2'} = 1/\sqrt{6}\,(\phi_{15} + \phi_{16} + \phi_{17} + \phi_{18} + \phi_{19} + \phi_{20})$$

$$\psi^{2}_{A_2'} = 1/\sqrt{6}\,(\phi_{1} + \phi_{4} + \phi_{11} + \phi_{14} + \phi_{5} + \phi_{8})$$

$$\psi^{3}_{A_2'} = 1/\sqrt{6}\,(\phi_{2} + \phi_{3} + \phi_{12} + \phi_{13} + \phi_{6} + \phi_{7})$$

$$\psi^{4}_{A_1''} = 1/\sqrt{6}\,(\phi_{15} + \phi_{17} + \phi_{19} - \phi_{16} - \phi_{18} - \phi_{20})$$

$$\psi^{5}_{A_1''} = 1/\sqrt{6}\,(\phi_{1} + \phi_{14} + \phi_{8} - \phi_{4} - \phi_{11} - \phi_{5})$$

$$\psi^{6}_{A_1''} = 1/\sqrt{6}\,(\phi_{2} + \phi_{13} + \phi_{7} - \phi_{3} - \phi_{12} - \phi_{6})$$

$$\psi^{7}_{E_a'} = 1/2\sqrt{3}\,(2\phi_{15} - \phi_{17} - \phi_{19} + 2\phi_{16} - \phi_{18} - \phi_{20})$$

$$\psi^{8}_{E_b'} = 1/2\,(\phi_{17} - \phi_{19} + \phi_{18} - \phi_{20})$$

$$\psi^{9}_{E_a'} = 1/2\sqrt{3}\,(2\phi_{1} - \phi_{14} - \phi_{8} + 2\phi_{4} - \phi_{11} - \phi_{5})$$

$$\psi^{10}_{E_b'} = 1/2\,(\phi_{14} - \phi_{8} + \phi_{11} - \phi_{5})$$

$$\psi^{11}_{E_a'} = 1/2\sqrt{3}\,(2\phi_{2} - \phi_{13} - \phi_{7} + 2\phi_{3} - \phi_{12} - \phi_{6})$$

$$\psi^{12}_{E_b'} = 1/2\,(\phi_{13} - \phi_{7} + \phi_{12} - \phi_{6})$$

$$\psi^{13}_{E_a''} = 1/2\sqrt{3}\,(2\phi_{15} - \phi_{17} - \phi_{19} - 2\phi_{16} + \phi_{18} + \phi_{20})$$

$$\psi^{14}_{E_b''} = 1/2\,(\phi_{17} - \phi_{19} - \phi_{18} + \phi_{20})$$

$$\psi^{15}_{E_a''} = 1/2\sqrt{3}\,(2\phi_{1} - \phi_{14} - \phi_{8} - 2\phi_{4} + \phi_{11} + \phi_{5})$$

$$\psi^{16}_{E_b''} = 1/2\,(\phi_{14} - \phi_{8} - \phi_{11} + \phi_{5})$$

$$\psi^{17}_{E_a''} = 1/2\sqrt{3}\,(2\phi_{2} - \phi_{13} - \phi_{7} - 2\phi_{3} + \phi_{12} + \phi_{6})$$

$$\psi^{18}_{E_b''} = 1/2\,(\phi_{13} - \phi_{7} - \phi_{12} + \phi_{6})$$

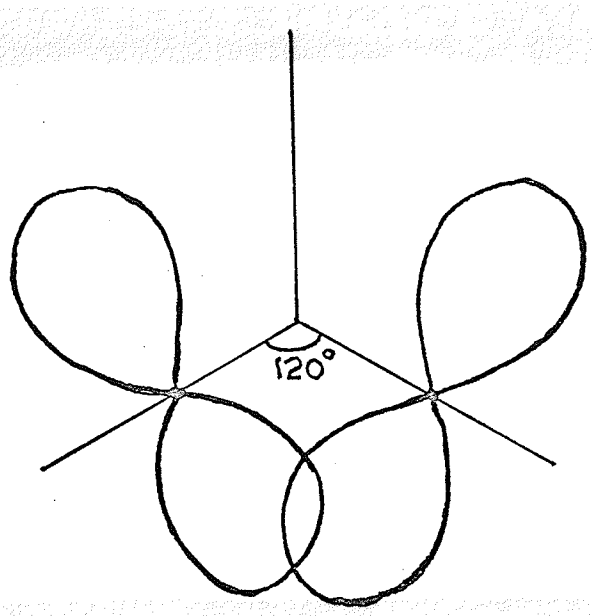

Figure 25: Inter-ring overlap of Class I p orbitals.

The energy level diagram is shown in Figure 26. The coefficients were then calculated from the secular equations and electron densities were calculated assuming the lowest nine energy levels filled. The electron densities are listed in Table XIII.

Table XIII

ELECTRON DENSITIES IN THE CARBON p - π ORBITALS

Positions	Electron density
1, 14, 8, 4, 11, 5	0.998854
2, 13, 7, 3, 12, 6	1.001052
15, 16, 17, 18, 19, 20	1.000094

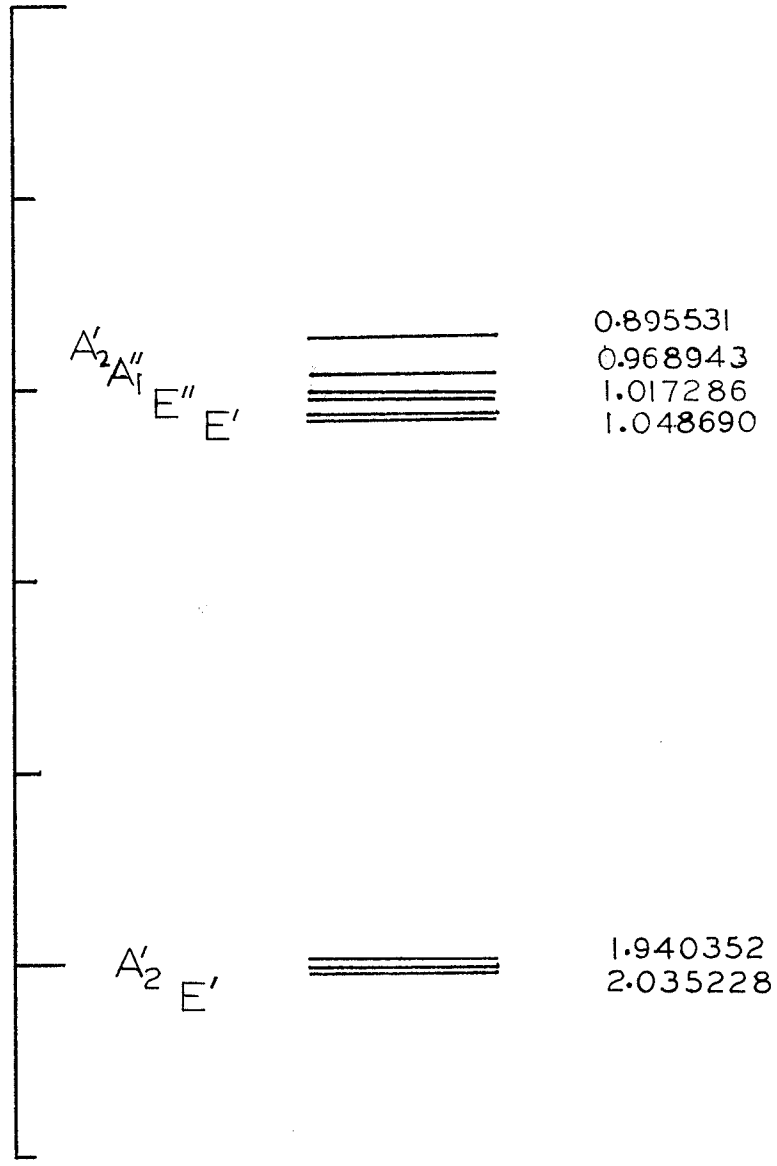

Figure 26: Energy level diagram of the p-π electron system of triptycene.

B - CALCULATION OF RING CURRENT SHIELDING

The ring current in the benzene molecule produces a magnetic field around the benzene molecule. Using the ring current model of Waugh and Fessenden (19), Johnson and Bovey (21) calculated the resulting shielding in p.p.m. as a function of the position measured in cylindrical polar coordinates.

The positions of the ring protons of one ring relative to an origin on one of the opposed rings were measured using trigonometric relations. The length of the C-C bond distance was taken to be 1.49 A^{o} and the C-H bond length 1.08 A^{o}. All distances were converted to ring radii (the length of the C-C bond and the unit of length used by Johnson and Bovey). The position of the bridgehead hydrogen relative to an origin on one of the rings was also measured. These values are summarized in Table XIV.

Table XIV

COORDINATE POSITIONS FOR ALL CLASSES OF TRIPTYCENE HYDROGEN RELATIVE AN ORIGIN ON ONE OF THE RINGS

Coordinate	Bridgehead H (ring radii)	A H's (ring radii)	B H's (ring radii)
ρ	2.48	3.48	3.14
z	0	2.83	1.50

The averaging process involved in the shielding effect renders negative and positive values on the "z" axis equivalent. The effect on the ring protons A and B of the two opposed rings is therefore double that due to a single ring. The shielding at the bridgehead proton is triple that due to a single ring. The tables of Johnson and Bovey give a value for σ' the shielding relative to benzene for values of ρ and "z" ranging from 0 to 4.00 in increments of 0.01. The values of σ' were calculated from the tables using the values of ρ and "z" given in Table XIV. Positive σ' corresponds to an increase in the apparent field and thus to a decrease in the applied resonance field and in τ,

$$\Delta\tau = -\sigma'$$

Values of σ' and $\Delta\tau$ are listed in Table XV.

Table XV

SHIELDING AT THE DIFFERENT CLASSES OF PROTONS IN TRIPTYCENE

	Bridgehead	A protons	B protons
σ'	+1.95	-0.04	+0.21
$\Delta\tau$	-1.95	+0.04	-0.21

BIBLIOGRAPHY

BIBLIOGRAPHY

1. J. W. Emsley, J. Feeney and L. H. Sutcliffe, "High Resolution Nuclear Magnetic Resonance Spectroscopy", Pergamon Press, (1965)
2. J. A. Pople, W. G. Schneider and H. J. Bernstein, "High Resolution Nuclear Magnetic Resonance", McGraw Hill Book Co. Ltd. (1959)
3. G. E. Pake, "Paramagnetic Resonance", W. A. Benjamin, New York (1962)
4. W. E. Lamb, Phys. Rev., 60, 817 (1941)
5. N. F. Ramsey, Phys. Rev., 78, 699 (1950)
6. N. F. Ramsey, Phys. Rev., 86, 243 (1952)
7. Reference 1, page 71
8. Reference 2, page 170
9. A. J. Dekker, "Solid State Physics", Prentice Hall Inc. (1957), page 27
10. L. Onsager, Phys. Rev., 37, 405 (1931)
11. L. Onsager, Phys. Rev., 38, 2265 (1931)
12. J. F. Nye, "Physical Properties of Crystals", Oxford (1957), page 41
13. J. A. Pople, Proc. Roy. Soc., A239, 550 (1957)
14. H. M. McConnell, J. Chem. Phys., 27, 226 (1957)
15. C. V. Raman, Nature, 123, 945 (1929)

16. L. Pauling, J. Chem. Phys., 4, 673 (1936)

17. K. S. Krishnan, B. C. Guha and S. Banerjee, Phil. Trans. Roy. Soc., A231, 235 (1933)

18. J. A. Pople, J. Chem. Phys. 24, 1111 (1956)

19. J.S. Waugh and R. W. Fessenden, J. Am. Chem. Soc., 79, 846 (1957)

20. J. S. Waugh, J. Am. Chem. Soc., 80 6697,(1958)

21. C. E. Johson Jr. and F. A. Bovey, J. Chem. Phys., 29, 1012, (1958)

22. F.London, J. Phys. Radium, 8, 397 (1937)

23. J. A. Pople, Mol. Phys., 1, 175 (1958)

24. H. J. Berstein, W. G. Schneider and J. A. Pople, Proc. Roy. Soc., A268, 328 (1962)

25. N. Jonathon, S. Gordon and B. P. Dailey, J. Chem. Phys., 36, 2443 (1962)

26. J. Hoaran, Ann. Chim., (Paris), 1, 560 (1956)

27. A series of papers by J. A. Pople on the molecular orbital theory of diamagnetism:

a) J. A. Pople, J. Chem. Phys., 37, 53 (1962)

b) J. A. Pople, J. Chem. Phys., 37, 62 (1962)

c) J. A. Pople, J. Chem. Phys., 38, 1276 (1963)

d) J. A. Pople, J. Chem. Phys., 41, 2559 (1964)

e) J. A. Pople, J. Chem. Phys., 42, 1560 (1965)

28. C. N. Banwell, "Fundamentals of Molecular Spactroscopy", McGraw-Hill Publishing Co. Ltd. (1966)

29. Reference 2, page184

30. Reference 1, page 103

31. H. M. McConnell, J. Mol. Spect., 1, 11 (1957)

32. H. M. McConnell, J. Chem. Phys., 30, 126 (1959)

33. A. D. Buckingham and K. A. McLauchlan, Proc. Chem. Soc., 144 (1963)

34. A. Saupe and G. Englert, Z. Naturforsch, 19a, 172 (1964)

35. L. C. Snyder and E. W. Anderson, J. Am. Chem. Soc., 86, 5023 (1964)

36. J. Martin and B. P. Dailey, J. Chem. Phys., 37, 2594 (1962)

37. C. N. Banwell, A. D. Cohen, N. Sheppard and J. J. Turner Proc. Chem. Soc., 266 (1959)

38. D. M. Grant, R. C. Hirst and H. S. Gutowsky, J. Chem. Phys., 38, 470 (1963)

39. P. F. Cox, J. Am. Chem. Soc., 85, 380 (1963)

40. R. Freeman, N. S. Bhacca and C. A. Reilly, J. Chem. Phys., 38, 293 (1963)

41. Reference 1, page 283

42. B. Dischler and W. Maier, Z. Naturforsch, 16A, 318 (1961)

43. J. A. Pople, W. G. Schneider and H. J. Bernstein, Can. J. Chem., 35, 1060 (1951)

44. B. Dischler and G. Englert, Z. Naturforsch, 16A, 1180 (1960)

45. T. K. Lim, A. Taurins and M. A. Whitehead, Can. J. Chem., 44, 1211 (1966)

46. J. H. Goldstein and G. S. Reddy, J. Chem. Phys., 36, 2644 (1962)

47. K. Ito, J. Am. Chem. Soc., 80, 3502 (1958)

48. N. Musher and D. E. Pritchard, J. Chem. Phys., 31, 768 (1959)

49. N. Musher and D. E. Pritchard, J. Chem. Phys., 31, 1471 (1959)

50. C. Juan and H. S. Gutowsky, J. Chem. Phys., 37, 2198 (1962)

51. D. M. Grant and W. M. Litchman, J. Am. Chem. Soc., 87, 3994 (1965)

52. M. Karplus and D. M. Grant, Proc. Nat'l. Acad. Sci. U.S., 45, 1269 (1959)

53. Cotton, "Chemical Applications of Group Theory", Interscience Publishers (1963), page 149

54. J. A. Pople, W. G. Schneider and H. J. Bernstein, Can. J. Chem., 35, 1060 (1957)

55. W. B. Smith and B. A. Shoulders, J. Phys. Chem., 69, 2022 (1965)

56. B. P. Dailey, J. Chem. Phys., 41, 2304 (1964)

57. C. Reid, J. Mol. Spect., 1, 18 (1957)

58. G. V. D. Tiers, 'Table of τ -Values for a Variety of Organic Compounds' in J. W. Emsley, J. Feeney and

L. H. Sutcliffe, "High Resolution Nuclear MagneticResonance Spectroscopy, Vol. II", Pergamon Press, Appendix B (1966)

59. "N. M. R. Spectra Catalogue", Varian Associates, (1962), Spectrum No. 201

60. R. S. Drago and N. A. Matwiyoff, J. Organometal Chem., 62 (1965)

61. H. Margenau and G. M. Murphy, "The Mathematics of Physics and Chemistry, Vol. II", D. Van Nostrand Company Inc. (1964), page 86